

DSIA JOURNAL

A Quarterly Publication of the Defense Systems Information Analysis Center

Volume 4 • Number 1 • Winter 2017

The MX/Peacekeeper and SICBM:

A SEARCH FOR SURVIVABLE BASING²²

4 In Situ Manufacturing of
**POLYMER NANOCOMPOSITES FOR
ENERGETIC APPLICATIONS**

11 **THE U.S. ROCKET PROPULSION
INDUSTRIAL BASE:**
A Status Report

17 Improved Capabilities in
GROUND TARGET TRACKING

35 **REAL-TIME, IN SITU
INTELLIGENT VIDEO ANALYTICS:**
Harnessing the Power of GPUs for
Deep Learning Applications



Distribution Statement A:
Approved for public release;
distribution is unlimited.

DSIAC JOURNAL

VOLUME 4 | NUMBER 1 | WINTER 2017

Editor-in-Chief: Ted Welsh

Copy Editor: Eric Edwards

Art Director: Melissa Gestido

On the Cover:

Photo Credit: Nuclear Missile Silo.

Photo Source: Steve Juvetson via Flickr Creative Commons.

The *DSIAC Journal* is a quarterly publication of the Defense Systems Information Analysis Center (DSIAC). DSIAC is a Department of Defense (DoD) Information Analysis Center (IAC) sponsored by the Defense Technical Information Center (DTIC) with policy oversight provided by the Assistant Secretary of Defense for Research and Engineering, ASD (R&E). DSIAC is operated by the SURVICE Engineering Company with support from Georgia Tech Research Institute, Texas Research Institute/Austin, and The Johns Hopkins University.

Copyright © 2016 by the SURVICE Engineering Company. This journal was developed by SURVICE, under DSIAC contract FA8075-14-D-0001. The Government has unlimited free use of and access to this publication and its contents, in both print and electronic versions. Subject to the rights of the Government, this document (print and electronic versions) and the contents contained within it are protected by U.S. copyright law and may not be copied, automated, resold, or redistributed to multiple users without the written permission of DSIAC. If automation of the technical content for other than personal use, or for multiple simultaneous user access to the journal, is desired, please contact DSIAC at 443.360.4600 for written approval.

Distribution Statement A: Approved for public release; distribution is unlimited.

ISSN 2471-3392 (Print)
ISSN 2471-3406 (Online)



CONTENTS

4 In Situ Manufacturing of Polymer Nanocomposites for Energetic Applications ▶
AM *Advanced Materials*

11 The U.S. Rocket Propulsion Industrial Base: A Status Report ▶
EN *Energetics*

17 Improved Capabilities in Ground Target Tracking ▶
MS *Military Sensing*

22 The MX/Peacekeeper and SICBM: A Search for Survivable Basing ▶
WS *Weapon Systems*

35 Real-Time, In Situ Intelligent Video Analytics: Harnessing the Power of GPUs for Deep Learning Applications ▶
AS *Autonomous Systems*

CONTACT DSIAC

Ted Welsh
DSIAC Director

DSIAC HEADQUARTERS
4695 Millennium Drive
Belcamp, MD 21017-1505
Office: 443.360.4600
Fax: 410.272.6763
Email: contact@dsiac.org ▶

WPAFB SATELLITE OFFICE
96 TG/OL-AC/DSIAC
2700 D Street, Building 1661
Wright-Patterson AFB, OH 45433-7403
Office: 937.255.3828
DSN: 785.3828
Fax: 937.255.9673

DSIAC CONTRACTING OFFICER REPRESENTATIVES

Peggy M. Wagner (COR)
96 TG/OL-AC
2700 D Street, Building 1661
Wright-Patterson AFB, OH 45433-7403
Office: 937.255.6302

DSIAC PROGRAM MANAGEMENT ANALYST

Marisiah Palmer-Moore
IAC Program Management Office (DTIC-I)
8725 John J. Kingman Road
Fort Belvoir, VA 22060-6218
Office: 703.767.9109

Brad E. Forch (ACOR)
U.S. Army Research Laboratory
RDRL-WM
Aberdeen Proving Ground, MD 21005
Office: 410.306.0929

MESSAGE FROM THE EDITOR



TED WELSH

Ever wonder how the Cold War and the nuclear arms race of the 1960s and '70s have continued to influence the U.S.

strategic defense

outlook? Both the United States and the Soviet Union developed and deployed intercontinental ballistic missiles (ICBMs) as a result. These ICBMs were initially deployed in land-based silos considered to provide “safe” or survivable basing options. In other words, these fixed targets had limited vulnerability concerns given the early ICBMs’ limited precision. But as second- and third-generation ICBM weapon systems developed, so did the precision of their strike capability, which has led to ongoing concerns regarding potential fratricide based on the strategic deployment of these missiles and their nuclear warhead payloads.

In our feature article this quarter, Eugene Sevin discusses the vulnerability of U.S. ICBM systems, land-based deployment strategies, and associated silo hardening. Various basing modes are discussed for existing ICBM systems’ survivability along with vulnerability hardening alternatives. Additionally, mobile basing insights are provided, recognizing the potential to leverage Ground-Based Strategic Deterrent (GBSD) hardening strategies and technologies.

The potential of nanotechnology to influence the energetic industry continues to tantalize propellant and explosive formulators. In Mike Fisher’s related article, he highlights the significant benefits and promise offered by ongoing advancements

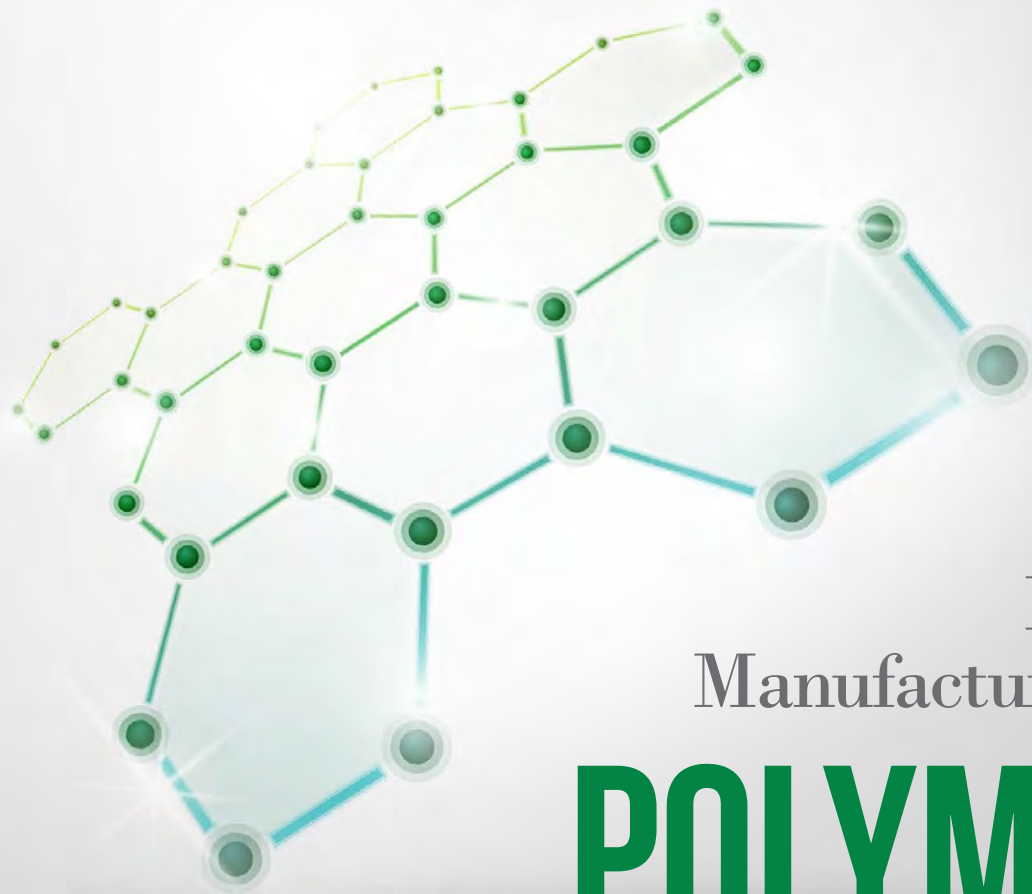
in nanoparticle polymer composites and processing, provided that related manufacturing challenges can be overcome.

Conversely, the U.S. rocket propulsion industry is facing numerous challenges that have weakened the associated infrastructure and workforce capability over the past 60 years. An aging workforce, oscillating budgets, manufacturing consolidation, obsolescence issues, and the dynamic complexities associated with foreign trade laws are limiting related technology advancements. However, there are some signs of resurgence, with increases in defense and space budgets highlighting the recognition for needed investment in rocket propulsion technology. Albert DeFusco’s article explores the infusion of capital investment on rocket propulsion industry and the associated positive impacts to the future of our defense preparedness and space travel.

Advancements in modeling and simulation (M&S) tools are also critical to maintaining our defense preparedness despite the increasing challenges of Department of Defense (DoD) budget constraints. M&S continues to be extremely important across all DoD acquisition-cycle phases, offering four major benefits: cost savings, accelerated schedule, improved product quality, and cost avoidance. This *DSIAC Journal* issue includes two articles that highlight two such M&S tools. Both tools identify evolving technology developments for improved situational awareness in a variety of intelligence, surveillance, and reconnaissance (ISR) scenarios, and with application to autonomous and weapons systems alike.

The first article—written by Teresa Selee, Jacqueline Fairley, and Ryan Hersey—highlights advancements in ground target tracking via a physics-compliant terrain scattering model that simulates the space-time statistics of radar returns from ground terrain as observed by an airborne radar. The M&S tool known as the Adaptive Sensor Prototyping ENvironment (ASPEN™) has recently been enhanced by the development of a ground target tracking module, and results are showing the value of the new modeling capability as a top-level indicator for vehicle and dismount tracking.

The second M&S-related article—written by Shawn Recker and Christiaan Gribble—deals with a convergence between deep learning technology and the use of computational algorithms to process visual and audio data. Sentinel™, a tool for real-time in situ intelligent video analytics (IVA), combines state-of-the-art techniques in high-performance computing (HPC), modern data reduction and analysis techniques, and deep learning to realize automatic target recognition (ATR), tracking, event detection, and other visually oriented tasks. This system leverages increased efficacy of deep neural networks in both image and speech recognition tasks, coupled with increased performance via graphics processing unit (GPU) acceleration, to support human-in-the-loop deployment scenarios and address ISR problems in defense, homeland security, disaster relief, emergency response, and even home security. ■



In Situ
Manufacturing of

POLYMER NANOCOMPOSITES

for Energetic Applications

By Michael Fisher

INTRODUCTION

For many years, propellant and explosive formulators have investigated the use of nanomaterials to increase performance and modify reactivity of energetic materials and related systems. The potential energetic performance enhancements offered by

nanoscale metal fuels include enhanced burning rates, easy ignition, higher specific impulse, improved combustion efficiency, and a greater potential for tuning performance through particle loading and size control [1–4]. The key advantages of a reduced particle size are tied to a high surface-to-volume ratio and short oxidation diffusion length, leading to enhanced reactivity. With nanoscale particles, the rate of reaction is determined by chemical kinetics

rather than mass transport. Oxide formation plays less of a role in controlling combustion rate. Consequently, the nanoparticles will react quickly at potentially lower temperatures than micron-scale particles. The nanoparticles are more likely to react completely rather than leaving behind unspent fuel with an oxidized shell. In some cases, these nanoparticles can increase the energetic yield of the system.

The small particle size can be a disadvantage, however, in that it creates new challenges with process scalability, long-term nanoparticle stability, safe handling, and particle agglomeration [1, 5, 6]. Because the particles are more reactive, they oxidize readily through contact with moisture and elevated temperature; they are subject to premature ignition by electrostatic discharge (ESD), impact, and friction; and they are nearly impossible to keep from agglomerating. Primary particle sizes on the order of 20 to 50 nm are not uncommon, but there is usually a notable size distribution with agglomerates on the order of 200 to 300 nm or greater. This size variation, which leads to performance variation, makes it extremely difficult to predict or control the particle morphology to better than a 50- to 100-nm resolution. Additionally, the loading levels of nanoparticles in a given system are limited, as their high surface area leads to drastic viscosity increases that hinder, and sometimes prohibit, mixing. Still, the promise for increased performance for energetics and power generation devices (such as batteries and fuel cells) drives continued investigation into new materials and processes.

In the energetics arena, the focus has mainly been on solid propellants, where the incorporation of nanoscale materials promises increased energy density and controlled energy release, while potentially improving sensitivity, environmental impact, and long-term stability. In addition to the current use of nanoparticles to increase propellant burning rates, and reduce agglomeration of aluminum (thereby increasing combustion efficiency through heat feedback to the burning surface and reduction of agglomerates in the exhaust), these materials may soon be used in radical new propellant

approaches that use three-dimensional nanostructures to control energy release and provide on/off capability. Such characteristics would be of great interest to explosives formulators and warhead designers as well [7].

In the energetics arena, the focus has mainly been on solid propellants, where the incorporation of nanoscale materials promises increased energy density and controlled energy release, while potentially improving sensitivity, environmental impact, and long-term stability.

POLYMER NANOCOMPOSITES

While the promise of the significant benefits of nanomaterials remains, capitalizing on these benefits has been somewhat elusive, primarily due to the lack of affordable, scalable processes for manufacturing high-quality nanoparticles in sufficient quantities to support high-volume production of nanomodified energetic materials.

There are many natural examples of organic and inorganic components combined at the nanoscale to construct materials with remarkable properties. Examples include bone, crustacean carapaces, and mollusk shells. Inspired by these natural materials, scientists

are developing new synthesis strategies to produce multifunctional nanoscale materials. In recent decades, material scientists have spent considerable effort investigating ways to combine an organic phase, typically a polymer, with inorganic nanoparticles, since research had shown that the addition of well-dispersed particles at the nanoscale allows significant tailoring of material properties, resulting in a new class of materials generally referred to as nanocomposites. Polymer nanocomposites, composed of solid, inorganic structures uniformly dispersed at the nanoscale in a polymer matrix, have taken on high importance in a variety of industries, as scientists gain the capability to define nanoparticle characteristics such as shape, size, uniformity of dispersion, and loading [8].

SYNTHESIS ROUTES

In general, polymer nanocomposites are prepared either by in situ synthesis of inorganic particles or by dispersion of fillers in a polymer matrix. The processing technique is critical to obtaining nanomaterials exhibiting the desired properties. Synthesis techniques are characterized as either bottom-up or top-down. In a top-down approach, nanoparticles are synthesized by breaking down bulk materials gradually into smaller sizes, or patterning using physical methods, such as the dispersion of layered silicates in polymer matrices. Examples of top-down processing include high-energy ball milling, cryochemical processing, and combustion synthesis [9].

Bottom-up methods, such as template synthesis, chemical (reactive) precipitation, chemical vapor deposition, supercritical fluid processing, and sol-gel synthesis, result in the buildup of nanoparticles atom by atom, or molecule

by molecule. In other words, precursors are used to construct and grow well-organized structures at the nanometric level.

Figure 1 illustrates the difference between top-down and bottom-up production processes in terms of their relative effects on material properties and performance.

Top-down methodologies have disadvantages associated with high cost and significant potential for damage to the nanoparticles produced. To achieve high-quality, affordable nanoparticles, bottom-up strategies seem to be the preferred approach. Generally, there are two methods used to produce bottom-up nanocomposites: (1) in situ polymerization in the presence of existing nanoparticles, or (2) in situ synthesis of inorganic nanoparticles in the presence of a polymer [8].

RECENT ADVANCES IN IN SITU NANOCOMPOSITE PROCESSING

Two examples of organizations currently using the in situ synthesis approach to produce polymer nanocomposites for energetic materials are the Helicon Chemical Company in Orlando, FL, and the Cornerstone Research Group (CRG) in Dayton, OH. These small businesses are involved in the research, development, and commercialization of advanced material and processing technology solutions to a variety of engineering problems. Each is independently researching and producing various nanoparticle-doped polymer systems using (in the case of

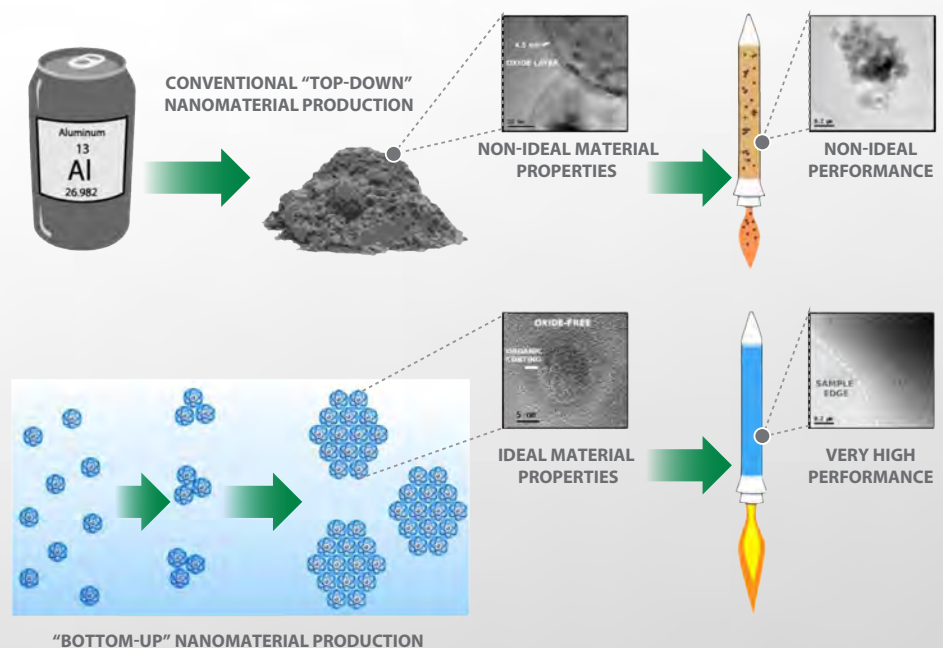


Figure 1: Bottom-Up vs. Top-Down Nanoparticle Production Approaches [10].

HTPB binders containing in-situ-grown nanoparticles can be used in conventional propellant production without modification.

Helicon) liquid-phase formation and (in the case of CRG) reactive gas-vacuum evacuation techniques. Between these organizations, a wide variety of particles can be produced on a scale large enough for large-scale propellant and explosive formulation. Helicon and CRG can produce materials in 200-g and kilogram-sized batches, respectively,

with further scale-up planned. Particles can be produced in polymer matrices with a wide variety of sizes, providing a solution to the formulation difficulties of introducing dry nanoparticles into propellant mixes.

Helicon has developed a liquid phase chemical process to grow nanoparticles in situ in existing polymer binders. The company's process uses optimized reaction conditions that allow polymers and nanoparticle molecular precursors to combine in single-phase solutions. The nanoparticles are then grown in situ by the bottom-up process of homogeneous nucleation. The nascent particles become coated by the surrounding polymer, which limits particle growth and prevents aggregation and agglomeration. This process generates homogeneous nanoparticle dispersions within the host polymer.

Because the nanoparticles are pre-formed in the polymer and never exist in a free state, the typical difficulties associated with nanoparticle mixing, handling, and safety are greatly reduced or eliminated [11].

For energetic materials applications, the company is developing products based on in-situ-grown nanoaluminum (nAl) and metal-oxide nanoparticles, such as TiO_2 . Hydroxyl-terminated polybutadiene (HTPB) R45M is the typical binder of choice for these materials, but the processes are adaptable to a wide variety of other polymers. The in situ nAl accelerates burning rates and increases combustion efficiency of solid fuels and propellants. By virtue of their small size, homogeneous dispersion, and lack of oxide coating, the nAl particles ignite and burn rapidly and completely. This nAl combustion provides intense heat feedback to the surface of the fuel or propellant, which accelerates the burning rate. By a different mechanism, TiO_2 increases the burning rate of composite propellants by catalyzing the gas-phase reactions of the oxidizer ammonium perchlorate (AP). The in-situ-formed TiO_2 particles have far greater specific surface area and dispersion uniformity than conventional nanopowders, which allows them to exhibit greater catalytic effect at lower particle loading. In both cases, the in situ nanoparticle-loaded liquid polymer/prepolymer binders are intended to be used as direct replacements for conventional binders (i.e., HTPB) in existing propellant mixing operations [11].

transmission electron microscopy (TEM) cross sections of cured HTPB binder containing the in situ nAl and conventional powdered nAl for comparison. The in situ binders are currently being produced at the hundreds of grams per batch scale, with near-term scale-up plans to kilogram-level in support of currently funded programs [10].

In a Navy-sponsored Small Business Innovation Research (SBIR) project, Helicon is developing an AP/HTPB composite propellant with equivalent performance to the double-base propellants currently used in ejection-seat rocket motors and cartridges [10]. The goal of this propellant development is to eliminate the safety hazard



Figure 2 shows the in situ nAl and TiO_2 in HTPB, while Figure 3 presents



Figure 2: In-Situ-Produced nAl in HTPB (top) and nTiO_2 in HTPB (bottom) [10].

Figure 3: Comparison of In Situ nAl With Conventional Micron Aluminum in HTPB [10].

associated with double-base propellant nitrate ester (NE) stabilizer depletion from prolonged high-temperature exposure, while duplicating, as closely as possible, performance of the incumbent propellant.

This new nanocomposite synthesis and processing technology is being used to create homogeneous nanoparticle/polymer composites. The propellant development effort combines multiple materials and technologies to achieve the desired effects. HTPB binders containing Helicon's homogeneous nAl and nTiO₂ produce composite propellants with the unique performance characteristics required for this effort. Table 1 lists the specific properties brought to the propellant formulation by each of the nanomaterials employed.

Formulations matching specific impulse, burning rate, plateau behavior,

temperature sensitivity, and thermal stability goals have been developed and tested. Current formulation efforts are focused on extending the burning rate plateau to a higher pressure regime. Figure 4 illustrates the significant increase in burning rate achieved using a relatively low loading of the novel nAl.

In contrast, CRG has adapted a much different in situ nanocomposite

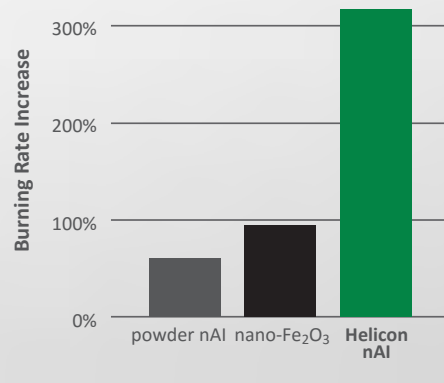


Figure 4: Effect of Helicon's nAl on Propellant Burning Rate [10].

manufacturing method to address the challenge of nanoparticle incorporation in a variety of energetic applications, including gun propellant, nanothermite, and rocket propellant applications. This process, depicted in Figure 5, converts an adsorbed gaseous precursor to the nanoparticles of interest using the molecular free volume of the polymer as a template. Typically, the particles are on the order of 5 to 10 nm in size, although it is possible to grow the particles larger by repeating the process. The particles are monodisperse, uniform in size and shape, and of high purity, provided that quality precursor materials are used. Because the particles form directly from the gas phase, already trapped in a polymer binder, there is no route for particle agglomeration and the particles are provided a degree of oxidation resistance.

In situ nanocomposite manufacturing replaces both the synthesis and mixing steps of traditional nanocomposite fabrication. The significant challenges associated with incorporating

Table 1: Properties of Al/HTPB Polymer Nanocomposites [10].

nAl DISPERSED IN HTPB	NTiO ₂ DISPERSED IN HTPB
Oxide-free	Highly active anatase crystal structure
Homogeneous dispersion in the binder	Homogeneous dispersion in the binder
Extremely rapid ignition	Effective at low concentration (~0.1%)
Complete combustion	High burning rates due to AP reaction catalysis
Not catalytic toward AP decomposition	
High burning rates due to heat feedback mechanism	

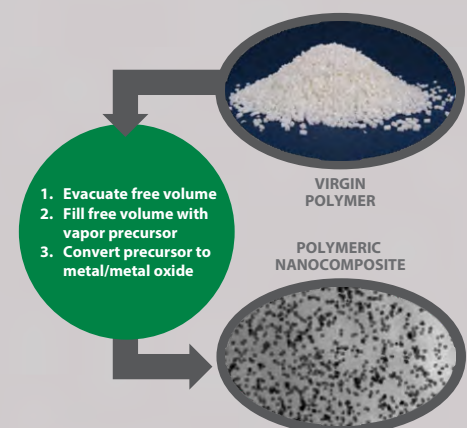


Figure 5: Solid Phase In Situ Nanocomposite Manufacturing Process [1].

nanoparticles into a polymer binder are eliminated because the nanoparticles form already dispersed in the polymer. A polymer matrix is used as a template for growing the particles in situ. There are no freestanding nanoparticles. They do not exist until they are trapped in a polymer that is easy and safe to handle. Figure 6 illustrates the basic configuration of CRG's nanomanufacturing system, in this case a reaction vessel designed for remote operation to allow evaluation of energetic polymers.

The in situ nanomanufacturing process is highly scalable. CRG can currently produce 1–5-kg batches, but there is equipment currently under development to allow larger-scale processing (including a large-scale reactor that will be able to process 30-kg batches).

In a Phase I SBIR effort with the U.S. Air Force Research Laboratory (AFRL), CRG has demonstrated the feasibility of using this in situ nanocomposite

manufacturing process to fabricate core-shell fuel and oxidizer materials to meet the military's future demands for high-energy density energetic material compounds for a variety of applications. This effort is expected to enable high-volume production of a material whose theoretical value has not been realized because of production limitations.

Successful processing of core-shell particles in multiple polymers, including cellulose acetate butyrate (CAB) and several fluoropolymers, has been reported. CAB was selected based on previous projects in which high-quality aluminum nanoparticles were produced with consistency. The fluoropolymers were selected as stable, high-temperature materials with high free volume and a ready supply of free-flowing powder to act as the template for nanoparticle growth.

On the AFRL-sponsored project, this nanocomposite processing method has been used to produce core-shell particle

morphologies with a technique that has already been demonstrated at 1-kg batch sizes and can easily be scaled to 100-kg and 1,000-kg batches. The core-shell structures have been imaged in the nanomodified fluoropolymer materials. It is believed that the core-shell particles were produced in CAB as well, but challenges with TEM sample preparation restricted the team's ability to image the particles in that polymer system. Particle size varies with the polymer matrix, and phase identification of the iron oxide is challenging in the characterization for all materials.

Early work on the formation of iron oxide on aluminum core-shell particles in a fluoropolymer binder has indicated success in forming some core-shell particles, as shown in Figure 7, while also forming particles of aluminum, iron, and what is thought to be an Al/Fe intermetallic compound.

While the feasibility of producing core-shell iron oxide on aluminum has been established, optimization of these materials is still needed. The core-shell nanothermite particles appear to vary in size, with the majority of particles measuring less than 25 nm. Particles produced include a mix of iron, aluminum, and core-shell morphologies. The particles appear well-dispersed and are already useful for tuning performance in energetic formulations containing polymer binder systems. Further characterization with TEM on these particles will confirm the phase identity of fuel and oxidizer, the relative ratios of core and shell chemistries, the particle formation process, and the size and distribution of particles. The

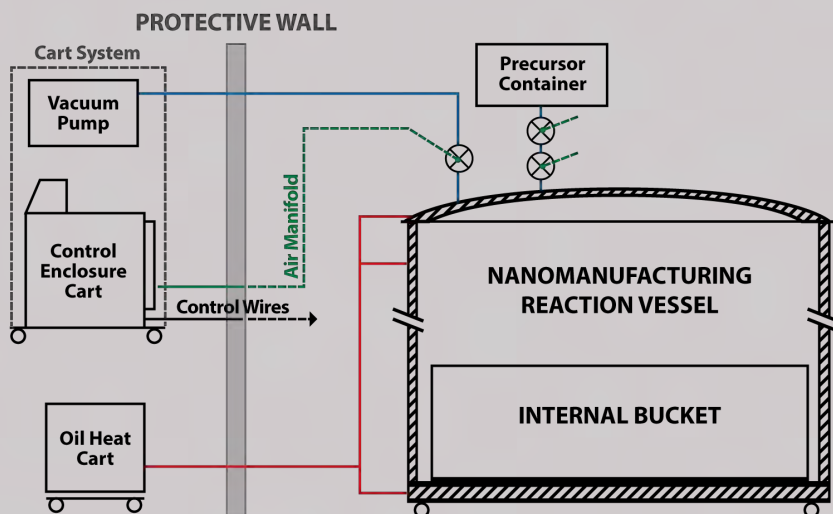
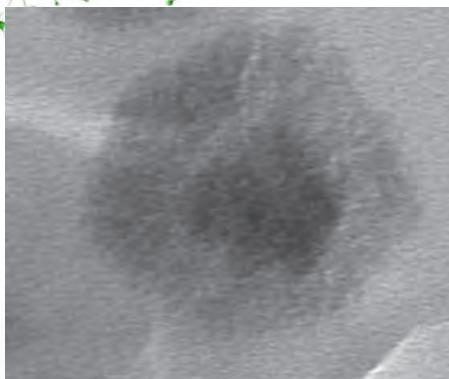


Figure 6: The CRG Nanocomposite Manufacturing System [12].



20 mm

Figure 7. Core of Aluminum Surrounded by Iron Oxide Shell [1].

oxidizer and fuel layers need further improvement through optimization of the current process conditions and possible pretreatment of the polymer.

FUTURE RESEARCH AND TECHNOLOGY COMMERCIALIZATION

Multiple Department of Defense organizations have expressed interest in these new nanocomposite manufacturing techniques and have funded research projects to evaluate the resultant nanomaterials in a range of potential applications. These applications include the aforementioned solid rocket propellants, as well as high explosives, solid gun propellants, solid fuels for ramjet combustors, and mitigation concepts to address insensitive munition (IM) requirements for fast and slow cookoff. Other applications have been proposed in the energetics arena, such as reactive materials for warhead liners and cases, as well as ignition materials with increased reactivity.

The Helicon technology was originally developed with energetic materials applications in mind, especially for the use of in situ nAl as a high-

performance fuel and propellant ballistic modifier. Much of the company's commercialization efforts remain focused in this area. These efforts include the development of new composite propellants with advanced performance characteristics, such as plateau burning propellants; hybrid rocket fuels; and IM. Benefits are also anticipated in explosives applications, and efforts are underway to adapt this process to liquid hydrocarbon fuels and hypergolic propellants.

Most of CRG's development work has likewise focused on various energetic materials applications. The company believes there is considerable promise in that space for tailoring burn rates, increasing energy density, improving combustion efficiency, and reducing sensitivity.

The ultimate commercialization potential of these high-quality, affordable, polymer nanocomposites, however, likely extends beyond energetics applications and into large market spaces, such as optical materials, solid electrolyte batteries, capacitors, photovoltaics, and fuel cells [11, 12]. ■

ACKNOWLEDGMENTS

The author gratefully acknowledges Dr. Michael Rauscher (Director of Advanced Materials at CRG) and Dr. David Reid (President of the Helicon Chemical Company) for their discussions and valuable input to this article.

REFERENCES

- [1] Rauscher, M., et al. "In Situ Nanocomposite Additives for Energetic Materials." Conference paper, Cornerstone Research Group, Dayton, OH, unpublished.
- [2] Ivanov, G.V., and F. Tepper. "Activated Aluminum as a Stored Energy Source for Propellants." Proceedings of the 4th International Symposium on Special Topics in Chemical Propulsion, 27–28 May 1996.
- [3] Lessard, P., F. Beaupré, and P. Brousseau. "Burn Rate Studies of Composite Propellants Containing Ultra-Fine Metals." 32nd International Annual Conference of ICT, Karlsruhe, Germany, 3–6 July 2001.
- [4] Risha, G. A., B. J. Evans, E. Boyer, R. B. Wehrman, and K. K. Kuo. "Nano-Sized Aluminum- and Boron-Based Solid-Fuel Characterization in a Hybrid Rocket Engine." 39th AIAA/ASME/SAE/ASEE Joint Propulsion Conference, Huntsville, AL, 20–23 July 2003.
- [5] Jones, D. E. G., R. Turcotte, R. C. Fouchard, Q. S. M. Kwok, A.-M. Turcotte, and Z. Abdel-Qader. "Hazard Characterization of Aluminum Nanopowders Compositions." *Propellants, Explosives, Pyrotechnics*, vol. 28, no. 3, pp. 120–131, 2003.
- [6] Park, K., A. Rai., and M. R. Zachariah. "Characterizing the Coating and Size-Resolved Oxidative Stability of Carbon-Coated Aluminum Nanoparticles by Single-Particle Mass-Spectrometry." *Journal of Nanoparticle Research*, vol. 8, pp. 455–464, 2006.
- [7] Schadow, K. "Energetics and Power Generation." *Nanotechnology Aerospace Applications*, Educational Notes RTO-EN-AVT-129, Paper 7, Neuilly-sur-Seine, France, 2005.
- [8] Oliveira, M., and A. V. Machado. "Preparation of Polymer-Based Nanocomposites by Different Routes." Institute for Polymers and Composites, University of Minho, Guimarães, Portugal, 2013.
- [9] "Nanomaterials and Nanotechnology." http://www.vscht.cz/sil/keramika/Ceramic_Technology/SM-Lect-14-A.doc, accessed November 2016.
- [10] Reid, D., E. Petersen, and S. Seal. "Development of Plateau Burning Composite Propellant for Ejection Seat CAD/PAD Systems." CAD/PAD Technical Exchange Workshop, May 2016.
- [11] Reid, D. Personal communication with author. 2016.
- [12] Rauscher, M. Personal communication with author. 2016.

BIOGRAPHY

MICHAEL FISHER is a senior staff engineer for DSIAC, specializing in propulsion, energetic materials, and weapons systems. During his 32-yr career, he has provided propulsion system design and program management support to a variety of Navy weapons programs and has managed propulsion and advanced materials research and development projects for a small business. Mr. Fisher previously supported both the NATO Munitions Safety Information Analysis Center (MSIAC) in Brussels and the Chemical Propulsion Information Analysis Center (CPIAC) as a technical specialist. He has presented numerous papers on propulsion design, IM, and energetics at conferences and workshops in the United States and abroad. Mr. Fisher has a B.S. in mechanical engineering from the University of Dayton.

The U.S. ROCKET PROPULSION INDUSTRIAL BASE

A Status Report

By Albert DeFusco

BACKGROUND

Rocket propulsion industrial base issues have spanned virtually every facet of the industry, as many officials and workers in the Department of Defense (DoD), the National Aeronautics and Space Administration (NASA), and contractor communities are well aware. Over the past 60 years (which comprises at least two generations of scientists and engineers), the industry has witnessed an aging workforce, oscillating budgets, consolidation among government facilities and contractors, obsolescence issues, and more complex and restrictive foreign trade laws. These changes have created a complex web of interrelated issues that are not easily documented and that cannot be easily resolved in the future by addressing each problem



individually. Many people believe that if rocket propulsion technology is to thrive in the coming decades, steps toward restoring defense and space budgets in all areas, as well as commitments to improving infrastructure and workforce capability, must be made.

One might suggest that the glamour of the past space race and the rocket propulsion industry may have run its course. Seeming to dampen the prospects for a bright future are a workforce with the majority of experienced scientists and engineers at or near retirement age, declining numbers of employees with advanced science and technology degrees, and a lack of newly degreed scientists and engineers pursuing and sustaining employment in the industry while seeking jobs in more appealing fields. For example, the field of energetic materials is considered to be more than 100 years old, with few significant discoveries or leaps in performance since the time of Ascanio Sobrero (when nitroglycerin [NG] was discovered in 1847) [1] and Georg Henning (when cyclotrimethylenetrinitramine [RDX] was discovered in 1898) [2]. Some experts even consider energetic materials to have reached their limit of performance until a new form of materials can be devised and used [3].

Declining budgets have necessitated a vast array of rationalizations at government laboratories and defense contractors. Reductions in facilities and workforces within the contractor communities have resulted in fewer people with critical skills, overcapacity and stagnant facilities, and fewer competitors. For example, the loss of the Space Shuttle program has catalyzed a number of reactions in the contractor community, including forcing thousands of reductions in the

skilled workforce, overcapacity in raw materials, and underused facilities at the subprime supplier levels. In addition, driving down the price of missiles and subcomponents at the prime level has created lower profit margins at the subprime level and has forced some small businesses to close, often leaving a void for critical materials and components that are difficult to reconstitute [4].

There is approximately one supplier for every two critical munitions components, reflecting a lack of competition and adequate depth at the subprime level.

Obsolescence issues continually surface as, for example, third-tier commercial material suppliers rationalize their portfolios of products that are no longer viable due to lack of demand or ever-increasing environmental regulations, the worst of which are unplanned. Reduced demand for unique materials that are specific to defense products and have no (or no longer satisfy) commercial needs have forced the defense industry to seek alternatives in a timely manner. As a result, rocket propulsion suppliers and prime contractors are continually faced with assessing new materials, which can force costly and time-consuming requalification, often at the suppliers' expense. One such material that presented an unplanned obsolescence issue about a decade

ago was butanetriol (BT), which resulted from a nearly depleted stockpile [4, 5]. The Office of the Under Secretary of Defense (OUSD), Acquisition, Technology and Logistics (AT&L) and the military services, along with suppliers, were instrumental in quickly developing new reliable sources for this critical material. Policies for handling obsolescence issues are needed as part of the DoD's projected budgets and planning.

However, all may not be lost. The OUSD AT&L is actively addressing these intertwined and complex issues. Dr. Chris Michienzi, Senior Industrial Analyst – Missiles and Munitions, OUSD(AT&L), Manufacturing and Industrial Base Policy (MIBP), presented this important topic at a meeting of the Critical Energetic Materials Working Group (CEMWG) in the spring of 2016 [5, 6]. Dr. Michienzi's "OSD Industrial Base Strategy" concisely outlined the dilemmas facing the defense industry and the steps that the OUSD is taking to help resolve them [7]. The mission of the MIBP is to "ensure robust, secure, resilient, and innovative industrial capabilities upon which the Department of Defense can rely to fulfill the Warfighter's requirements." As shown in Figure 1, a three-pillared approach is being used to assess the state of the nation's industrial base and ensure adequate manufacturing capabilities for goods and services to support U.S. defense needs.

This needed approach reflects the high degree of uncertainty in the defense industrial base and its ability to design, manufacture, and sustain present and future DoD critical capabilities. The uncertainty is demonstrated by the many defense budget swings since 1948, as illustrated in Figure 2. These swings have led to industry consolidations, workforce reductions, loss of critical

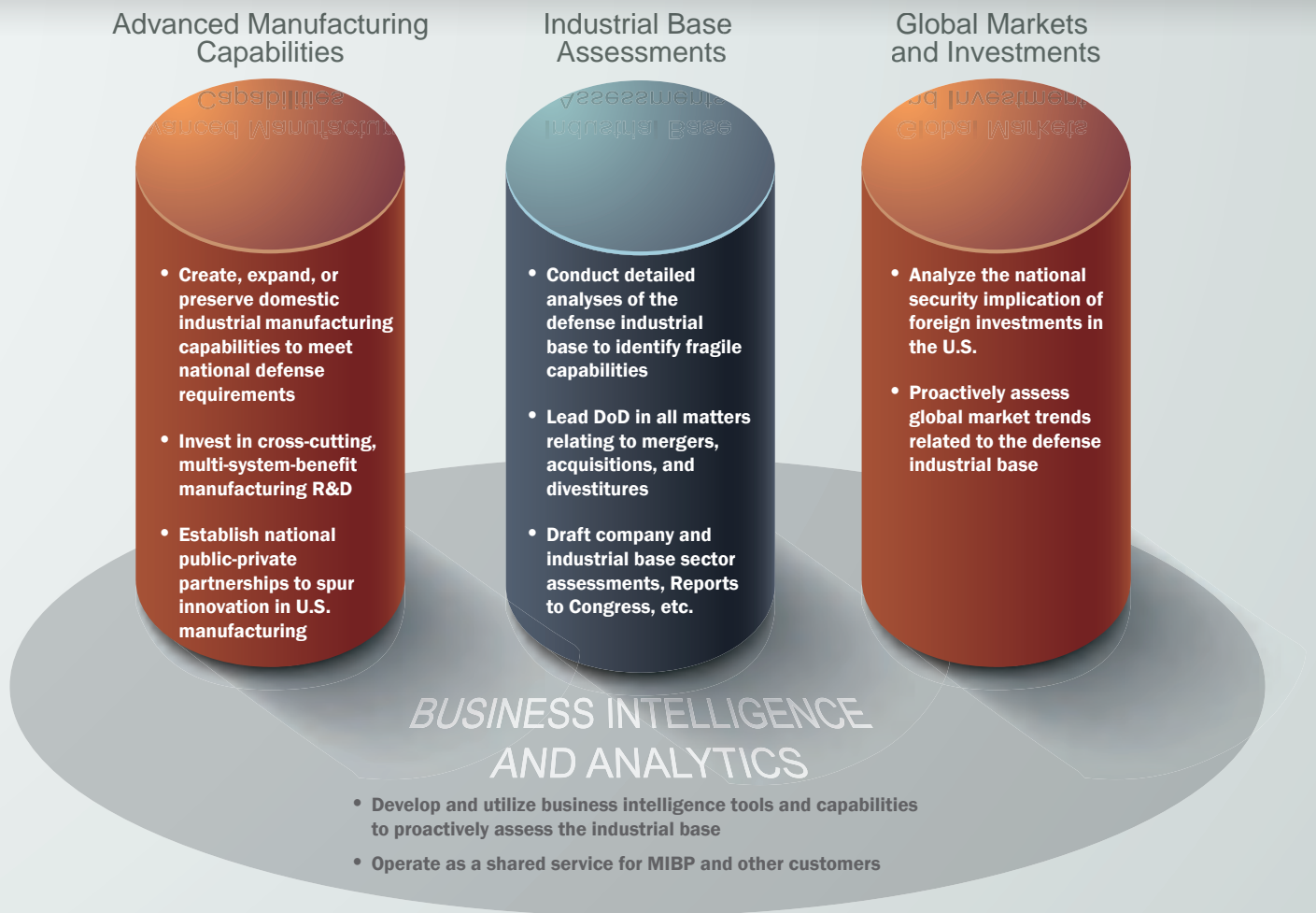


Figure 1: Approach to U.S. Industrial Base Assessment and Manufacturing Capability Assurance.

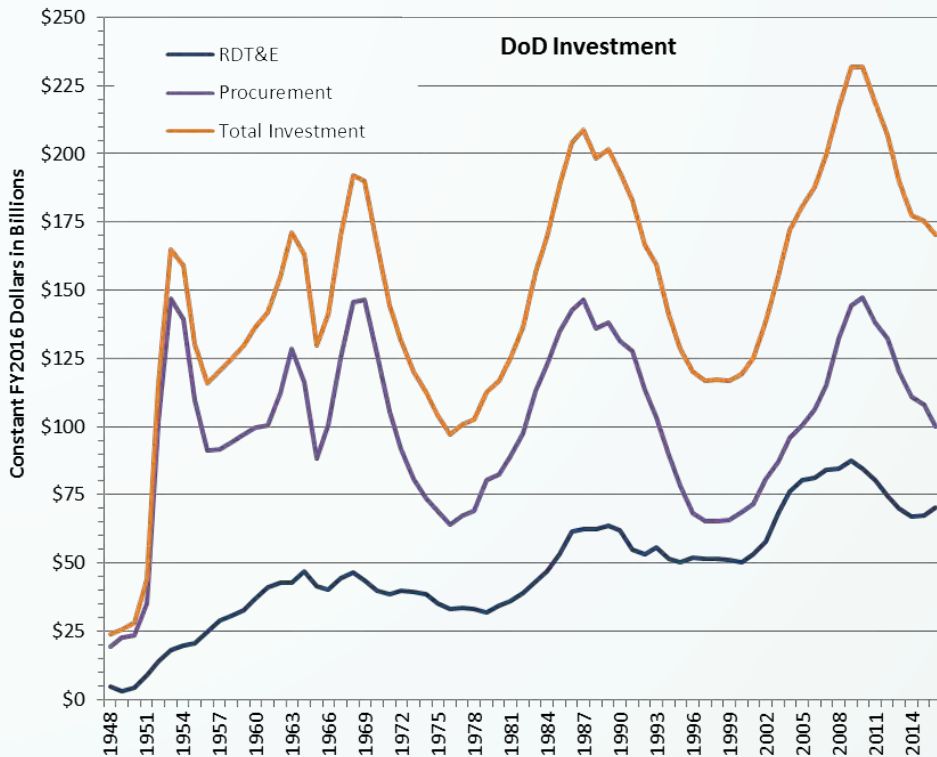
skills, the inability to plan for future business, lack of surge capability, and aging and stagnant facilities, all of which represent a general deterioration of the industry.

Since the end of World War II, the industry has become reactionary, rather than progressive, out of necessity. As Dr. Michienzi points out, the industrial base has experienced a multitude of consolidations even as recently as 1980, where 300 viable companies have been reduced to only 5 prime contractors through acquisitions, mergers, and closures. Likewise, over the past several years, five or so key second-tier rocket propulsion contractors have now been reduced to two continental United States (CONUS) companies [4]. Meanwhile,

an influx of foreign companies securing operation of critical plants in the United States proves that the rocket propulsion and ammunition industrial base has been “globalized” [8, 9]. Furthermore, critical components for munitions are dominated by single- or sole-source second-tier and third-tier suppliers. Interestingly, there is approximately one supplier for every two critical munitions components, reflecting a lack of competition and adequate depth at the subprime level, where most of the issues previously discussed reside. In contrast, prime contractors are considered “generally healthy.”

Although these changes in the defense industry are the result of justifiable business decisions, the OUSD’s MIPB

activities seek to create competition by encouraging new entrants into the supplier base and helping to mitigate loss of critical capabilities in the future. For example, the OUSD through Industrial Base Analysis and Sustainment (IBAS) funding is now supporting the creation of a second source for a critical material, hydroxyl-terminated polybutadiene (HTPB), which is used extensively in the defense and space industries [10]. Through the OUSD and CEMWG actions, continued emphasis will be placed on identifying at-risk critical materials, while creating better policies and plans and helping to seek funding for subprime and small business contractors to address material obsolescence and sole-source issues.



Source: National Defense Budget Estimates for FY 2015 (Table 6-11)
http://comptroller.defense.gov/Portals/45/Documents/defbudget/fy2015/FY15_Green_Book.pdf

Note: All enacted war and supplemental funding is included.

Figure 2: The Ups and Downs of the U.S. Defense Budget Over the Last Half Century.

One bright spot for the future of the U.S. rocket propulsion industry (along with the greater aerospace industry) is the increased participation in, and support of, U.S. science, technology, engineering, and mathematics (STEM) initiatives. In these programs, students are exposed to design and implementation challenges and can compete for scholarship awards [11–14]. New scientists and engineers will face the challenges of going beyond their field of training and working in a more multi-disciplinary environment, which STEM encourages through local middle schools, high schools, and colleges. The intent of revitalizing the aerospace and defense industries through STEM may be realized when the next generation of scientists and engineers enters the workforce.

The FY17 National Defense Authorization Act (NDAA) may be another bright spot. This legislation authorizes funding across all aspects of the industry and focuses on rebuilding our nation's defense in many ways [15]. As stated in the introduction to House Armed Services Committee (HASC) Communication 52539, "Unprecedented threats, uncertainty, and technological change, combined with a high-operational tempo and declining resources, have sharply eroded the readiness of our military" [16]. The bill was brought to the floor of the House of Representatives by HASC Chairman William Thornberry in April 2016 and was subsequently passed by the House in May 2016. After revisions, joint House-Senate committee approvals, and

The future of the U.S. defense industrial base also holds some promise for innovation and the development and application of new technologies where small businesses and competition may be key factors for future expansion.

signings by both the House and Senate, the bill was presented to the President and signed into law on 23 December 2016 [17].

The DoD discretionary base budget of the FY2017 NDAA is valued at \$523.7 billion, which exceeds the February 2015 base cap of \$523.1 billion agreed upon by Congress [18]. The budget restores military readiness and shortfalls in many areas of defense, including critical munitions (such as the Javelin, Guided Multiple Launch Rocket System [GMLRS], Army Tactical Missile System [ATACMS], Hydra 70, and AIM-9X Sidewinder missiles). In addition, the Army and Navy will obtain the new Joint Air-to-Ground Missile (JAGM) to eventually replace the current Hellfire missile system. The bill provides funds for procurement of 100 Tomahawk missiles for the Navy to sustain manufacture and reduce risk to the industrial base for this missile. The Army will also be provided with \$242 million for Production Base Support at industrial facilities, reflecting



Tomahawk Block IV cruise missile during a flight test (U.S. Navy).

a need to maintain and revitalize manufacturing sites across the United States.

Another interesting aspect of the bill addresses foreign military sales (FMS). The HASC originally commented on this topic by stating that the “hyper-bureaucratized process for selling military equipment to foreign militaries” limits the “United States’ ability to develop the capabilities of partners and allies around the world.” The bill requires the review of the DoD’s role in the FMS process in great detail to introduce reforms.

Other items, such as the forgoing retirement of A-10 aircraft and increasing projections for the aircraft carrier fleet and other aircraft and helicopters, will certainly help in providing future business for propulsion

and munitions suppliers. Modernization of the nuclear weapons stockpile and improved maintenance are also proposed, rather than following the President’s recommendation to accelerate retirement of these weapons. Continuation of the preliminary design concept and technology maturation phase for the future combined Ground Based Strategic Deterrent (GBSD) program is provided to consolidate U.S. ballistic missile defense capability and reduce risk to the program. The HASC originally recommended that the Air Force carefully consider its acquisition strategy, while promoting full and open competition, for the GBSD program since it will have “lasting impacts on the health and vitality” of the defense industrial base. The bill also establishes no new Base Realignment and Closure (BRAC) in 2019, which reflects support for maintaining current defense-related

capabilities and possibly the workforce. In addition, the bill requires the DoD to develop a new missile defeat strategy, including ballistic missile and cruise missile defense, and provides funds for Israeli missile defense systems.

The future of the U.S. defense industrial base also holds some promise for innovation and the development and application of new technologies where small businesses and competition may be key factors for future expansion. As stated in the HASC report on HR 4909 [15]:

“In the area of defense acquisition reform, H.R. 4909 seeks to create an engine of experimentation and innovation within the core acquisition system, while further strengthening acquisition planning and accountability. Specifically, the bill requires major

defense acquisition programs, to the maximum extent practicable after January 1, 2019, to be designed with modular, open-system approaches that enable weapon system components to be more easily upgraded as technology and threats evolve. The bill authorizes the military services, rather than specifying projects two years beforehand through the traditional budget process, to budget flexible funds with which to experiment with and rapidly field emerging technologies during the year of execution. It aligns intellectual property rights to an open-system approach and rebalances property rights so the government continues to receive necessary technical data while encouraging companies to do business with the Department.”

These statements, along with the information provided previously, support the hopeful revitalization of the defense industry, encourage growth and competition among defense suppliers, protect property rights, advance technology, and leverage newly discovered technologies as quickly as possible. ■

REFERENCES

- [1] Fant, Kenne. *Alfred Nobel: A Biography*. Arcade Publishing, 1993.
- [2] Henning, Georg. German Patent No. 104280, June 1899; see also <https://en.wikipedia.org/wiki/RDX>, accessed November 2016.
- [3] Ciezak-Jenkins, Jennifer A. “Disruptive Energetics-Fundamental Science for the Future.” U.S. Army Research Laboratory presentation, 27 April 2016.
- [4] Read, Robert M. “Solid Rocket Motor (SRM) Congressional Interest.” Office of the Under Secretary of Defense for Acquisition, Technology and Logistics presentation, 1 December 2009.
- [5] Olson, David. “Critical Energetic Material Initiative.” Presentation at the 2012 Insensitive Munitions and Energetic Materials Technology Symposium, 16 May 2012.
- [6] U.S. Department of Defense. “MIBP: Manufacturing and Industrial Base Policy.” <http://www.acq.osd.mil/mibp/>, accessed November 2016.
- [7] Michienzi, Chris. “OSD Industrial Base Strategy.” Presentation at the Critical Energetic Materials Working Group meeting, May 2016.

[8] BAE Systems. “Radford Army Ammunition Plant.” <http://www.baesystems.com/en-us/product/radford-army-ammunition-plant>, accessed November 2016.

[9] BAE Systems. “Holston Army Ammunition Plant.” <http://www.baesystems.com/en-us/product/holston-army-ammunition-plant>, accessed November 2016.

[10] DeFusco, Albert. “Historical Overview of HTPB: The Military’s Preferred Solid Propellant Binder for a Half Century.” *DSIAC Journal*, vol. 3, no. 4, October 2016.

[11] U.S. Department of Education. “Science, Technology, Engineering and Math: Education for Global Leadership.” <http://www.ed.gov/stem>, accessed November 2016.

[12] English, Lyn, Donna King, Peter Hudson, and Les Dawes. “iSTEM: The Aerospace Engineering Challenge.” *Teaching Children Mathematics*, vol. 21, no. 2, September 2014; see also <http://eric.ed.gov/?id=EJ1040289>, accessed November 2016.

[13] Orbital ATK. “Orbital ATK Scholarship Program Awards \$135,000 to 70 Students.” <https://www.orbital-atk.com/news-room/insideOA/2016Scholarship/default.aspx>, accessed November 2016.

[14] Raytheon. “Engaging Students with MathMovesU.” <http://www.raytheon.com/responsibility/stem/index.html>, accessed November 2016.

[15] 114th Congress, 2nd Session, House of Representatives. “National Defense Authorization Act for Fiscal Year 2017.” Report 114-840, 30 November 2016.

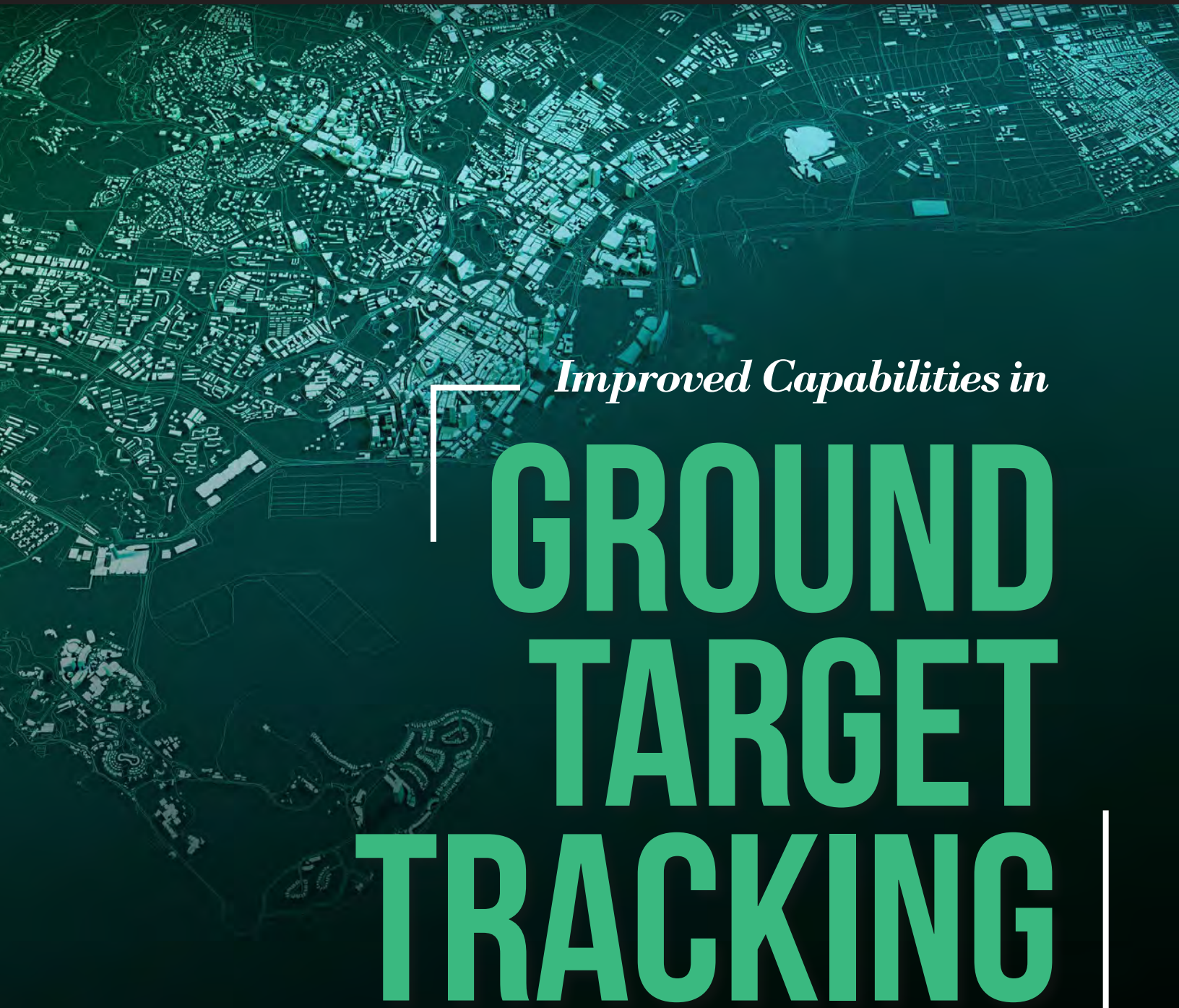
[16] House Armed Services Committee. “H.R. 4909 – The National Defense Authorization Act for Fiscal Year 2017.” Communication 52539, 2016.

[17] “S.2943 (114th): National Defense Authorization Act for Fiscal Year 2017.” <https://www.govtrack.us/congress/bills/114/s2943>, accessed 6 January 2017.

[18] Towell, Pat. “Fact Sheet: Selected Highlights of the FY2016 Defense Budget Debate and the National Defense Authorization Acts (H.R. 1735 and S. 1356).” Congressional Research Service report RR44019, 4 December 2014.

BIOGRAPHY

ALBERT DEFUSCO is currently a senior scientist at the SURVICE Engineering Company and a DSIAC subject-matter expert in energetic materials. He recently retired from Orbital ATK, where he spent 30 years in various capacities, including propellant and warhead formulating and energetic material synthesis. He also held various management positions in Orbital ATK’s Program Office and Engineering Departments. He started his career as a National Research Council post-doctoral fellow at the Naval Weapons Center (NWC) in China Lake, CA, and also worked in NWC’s Polymer Science Branch of the Research Department. Dr. DeFusco has a Ph.D. in organic chemistry from the University of Vermont and a B.S. in chemistry from the Worcester Polytechnic Institute.



Improved Capabilities in

GROUND TARGET TRACKING

By Teresa Selee, Jacqueline Fairley, and Ryan Hersey

BACKGROUND

Ongoing research at the Georgia Tech Research Institute (GTRI) has resulted in the development of a ground-target tracking module (GTTM) for the MATLAB®-based Adaptive Sensor Prototyping ENvironment (ASPEN™).

ASPEN™ is GTRI's primary tool for modeling and simulating airborne and space-based radar operation and assessing target detection and parameter estimation performance. It is a physics-compliant terrain scattering model that simulates ground returns by employing a large number of discrete

point scatterers judiciously positioned and spaced to replicate the space-time statistics of radar returns from terrain, as observed by an airborne radar. The model was originally created to support Space-Time Adaptive Processing (STAP) technique development.

Early versions of the model included prediction and benchmarking of ground moving target indication (GMTI) detection and estimation system performances, as well as the generation of synthetic data sets for algorithm maturation and refinement. In recent years, the simulation environment has been augmented to support a variety of modes and missions, such as air-to-air modes for airborne fire-control radars, wide bandwidths, and long dwell modes for systems such as synthetic aperture radar, urban operations, coherent change detection as observed from multi-pass collections, persistent surveillance, dismount detection and characterization, space-based operations, bistatic and multi-static implementations, electronic attack and electronic protection, radar operation from small unmanned aerial vehicles, and multiple simultaneous waveform transmission.

Additionally, the model has been extended to accommodate arbitrary waveforms and “true-time” referencing, which allows measured data files containing I/Q time samples to be read into the simulation environment and used as templates for radar returns from targets and ground clutter scatterers. ASPEN™ has also been extensively validated against test data collected from several radar systems operating from ultra high frequency (UHF) up through the Ku band, providing a high level of confidence in its representation of radar phenomenology.

ASPEN™ Structure

ASPEN™ functionality may be partitioned into two operations: synthesis and analysis. Synthesis is the generation of data realizations and signal statistics using high-fidelity models of the radar system and environmental effects. Data realizations are normally data cubes with dimensions assigned to the number of channels, slow-time pulses, and fast-time sample/range bin. Signal statistics are typically represented as space-time

ASPEN™ checks whether a given patch is shadowed by intervening terrain; if not in a shadow, the terrain type and grazing angle for the patch is used to determine reflectivity and, from the radar range equation, average power.

covariance matrices. Simulated targets can include moving ground and airborne vehicles, stationary discretely distributed surface clutter, jamming, and thermal noise.

Analysis includes a variety of classical and modern spectral estimators for diagnostics; a complete set of deterministic and adaptive GMTI filtering architectures; and calculators for statistical and stochastic benchmarking measures, such as signal-to-noise ratio (SNR), signal-to-interference-plus-noise ratio and related losses, probability of

detection, probability of false alarm, and Cramér-Rao Lower Bounds on the estimation error for various target parameters.

The baseline environment has modules for post-filter processing of synthetic and measured data, including a variety of constant false alarm rate detectors and direction-of-arrival estimators. Recent improvements to ASPEN™ include the ability to capture wideband and long-dwell phenomenology, as well as other enhancements, allowing performance benchmarking and data processing of multi-channel synthetic aperture radar (SAR) implementations. Graphical user interfaces (GUIs) have also been developed to facilitate the operation of ASPEN™ derivatives tailored to specific projects.

Synthetic Clutter Generation

The principal product of ASPEN™ for a source of interest is a data cube, a complex (I and Q) record as a function of fast-time (pulse repetition interval), slow-time (over the coherent processing interval), and channels. A separate data cube is formed for each signal source; these cubes are then coherently combined as the user desires, consistent with the assumption of linear superposition at the radar. Signal sources include external and internal thermal noise, distributed ground and ocean clutter, ground-based discrete scatterers, primary moving targets of interest, secondary “nuisance” targets, noise jammers, coherent jammers, and dismount signatures.

Distributed clutter is the most challenging signal source for data cube generation. Fundamentally, distributed clutter is modeled as a large number of stationary discretely known as

“clutter patches.” A precalculation step establishes the number and properties of these patches. By defining the scenario, the user implicitly influences the size of the area modeled with patches. For example, if the scenario is a fine-resolution, spotlight SAR collection, small patches might be defined and constrained to mainbeam angles and swath ranges only. Alternatively, for a medium-pulse-repetition-frequency mode where range- and Doppler-ambiguous clutter is a concern, larger patches will likely be defined for all angles from nadir to horizon.

Each clutter patch is modeled as a point-like scatterer, with the phase drawn randomly from a uniform distribution and the amplitude drawn from a Rayleigh distribution. The Rayleigh mean for a patch is set to a level consistent with the average clutter power at that location. The clutter reflectivity used to determine average power is a function of operating frequency, local grazing angle, and land type. Each clutter facet also has a deterministic spatial and temporal response, the former a function of the elevation and azimuth angle to the facet and the location of the receive channel phase centers, and the latter determined by the pulse-to-pulse phase progression generated by the relative motion of the sensor platform.

The default ASPEN™ mode of operation represents distributed clutter with a spherical, “sandpaper” earth—that is, the reflectivity model is a constant-gamma function with gamma invariant over all slant ranges and azimuth angles. The site-specific implementation, in contrast, uses digital elevation information to construct a true three-dimensional model of clutter patch locations and orientations. In this mode,

ASPEN™ checks whether a given patch is shadowed by intervening terrain; if not in a shadow, the terrain type and grazing angle for the patch is used to determine reflectivity and, from the radar range equation, average power.

Until now, there has been no “quick-look” capability to help assess big-picture, system-of-systems performance with “generic” GMTI track capabilities.

GTTM DEVELOPMENT

GMTI signal processing is typically developed for specific radar data collections or simulations. Until now, there has been no “quick-look” capability to help assess big-picture, system-of-systems performance with “generic” GMTI track capabilities. Recent research helped to fill this gap by implementing a novel signal processing chain and developing a tracking module with six different tracking architectures [1]. An accepted set of baseline tracking algorithms with adjustable parameters facilitates faster and more reliable analysis of problems of interest.

GTTM Technical Approach

Experience gained from processing both measured and simulated data was leveraged. Signal processing algorithms were implemented to process ASPEN™ raw detections. New outputs for this new module include tracks and associated metrics.

Initial parameters for the tracking architectures were chosen based on simulated vehicle motion; however, parameters may be adjusted for other datasets, scenarios, and operating environments. Realistic ground moving target scenarios were implemented using MATLAB. A user-friendly, visually interactive target/vehicle scenario module was developed to provide an interactive graphical approach for direct addition of trajectory data samples. Samples are created in the East-North-Up coordinate system on a high-resolution Google Map™ terrain figure. The open-source MATLAB script, Plot Google Map, was obtained from the MathWorks® file exchange and incorporated to generate terrain plots [2].

Accommodations of various ground-based environments are provided since the module is scripted to accept minimum and maximum latitude and longitude values. Operating within the defined terrain figure, the user can outline the desired ground target motion via a simple computer mouse click. To ensure all user-defined target motion inputs follow physical constraints and match real-world behavior, only user inputs falling within the specified maximum velocity constraint and revisit increment interval are accepted. Lastly, the target motion scenario is processed to obtain the detection performance in a simulated radar environment. These detections are processed as input measurements by the specified tracking architecture.

Six tracking architectures were developed with different initial parameters and levels of complexity. These six code bases provide options for comparisons and quick-look results. Additionally, they form the basis for developing problem-specific tracking. The codes can be grouped according

to the type of filter, level of complexity, or target(s) of interest. Grouping by filter type, three codes employ a single Extended Kalman Filter (EKF) to estimate track motion. The other three codes use an Interacting Multiple Model (IMM) of two EKFs; the two EKFs have different process noise values (one is conservative, and one allows for more uncertainty). Similarly, the six codes can be grouped according to the levels of complexity. The simple versions assume there are no features associated with measurements. The alternate version does include potential features (e.g., radial velocity, SNR, etc.) to adjust the size of the data association gate. Finally, the codes can be sorted based on the target class of interest. Four of the codes operate only on vehicles, while the other two operate on vehicles and dismounts and include an additional EKF for those detections classified as dismounts.

All six code bases exhibit the same structure regarding variables and general architecture. First, all tracks require a set number of detections similarly located to form a firm track—the required number is an input into the tracking module. At each time step, current measurements are compared to existing tracks to determine if they should associate with a track or start a new track. Additional logic determines whether a track should be labeled as tentative, firm, or dropped.

GTTM Development Results

Two examples of tracks generated by the new ASPEN™ module are provided in this section. In the first scenario, four vehicles move outward from the same location at the center of the scene, as shown in Figure 1. The detections (magenta indicating inbound targets and yellow representing outbound targets)



Figure 1: Scenario 1 - Radar Detections, Truth Data, and Platform Position Overlaid on a Terrain Map.

and truth (cyan) for four vehicles are overlaid on the Google map©. The green dots indicate the radar platform position. This figure is a snapshot in time, showing all detections up to that point. The x- and y-axis display longitude and latitude, respectively, both measured in degrees.

Vehicle tracking results (Scenario 1 with the IMM architecture) are illustrated in Figure 2. Detections are shown in cyan. Each of the four tracks is indicated with a different color, and a black asterisk designates the beginning of each track. Platform positions are updated and numbered in the order in which they appear. SNR and radial velocity are used in the data association process, as is the estimated target class (human, vehicle, animal, or clutter). Four tracks, with track lengths ranging from 20 to 45 track-state updates, are shown. For this scenario, track updates occur at 0.5-Hz intervals, and track lengths of 40 to 90 s

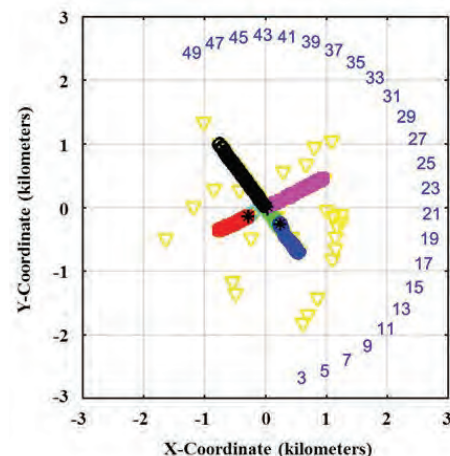


Figure 2: Tracking Results for Scenario 1.

are observed for a scenario lasting a total of 100 s.

An example scenario comprising a single vehicle driving a complex road network is shown in Figure 3.

EKF tracking architecture results are illustrated. The simple architecture



Figure 3: Detections (Shown in Magenta and Yellow) and Truth (Shown in Cyan) for a Single Vehicle.

assumes there are no features such as SNR or radial velocity to aid in the data association process. Target class (human, vehicle, animal, or clutter) is not included. A single track, with a track length of 63 track-state updates, is observed. For this scenario, track updates occur at 0.5-Hz intervals, yielding a track length of 126 s for a scenario lasting a total of 130 s. A view of the track is depicted in Figure 4.

CONCLUSIONS

The development of a flexible GMTI tracking capability in the ASPEN™ modeling environment is adding “big-picture” assessment to robust modeling of GMTI environments, architectures, and algorithms. In addition, the various advancements that this capability incorporates—including the creation of realistic simulated data sets via an interactive graphical approach, the

establishment of a signal-processing architecture to support the tracking functionality, the development and implementation of a tracking module comprising six different track filters, the simulation of realistic vehicle detections, etc.—are proving the value of this tool for continued development and analysis of GMTI tracking functions. ■

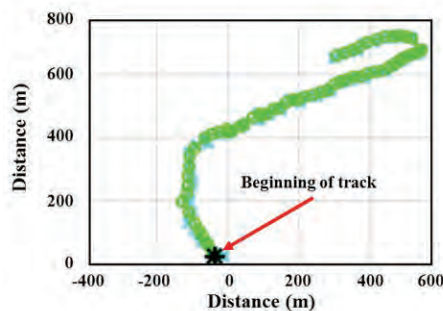


Figure 4: Zoom-In View of Simulation for Previously Depicted Scenario (Detections in Cyan; Tracks in Green).

REFERENCES

- [1] Hersey, R. K., and E. Culpepper. “Radar Processing Architecture for Simultaneous SAR, GMTI, ATR, and Tracking.” IEEE Radar Conference, May 2016.
- [2] The MathWorks. “Plot Google Map,” <http://blogs.mathworks.com/pick/2012/05/04/plot-google-map/>, accessed February 2016.

BIOGRAPHIES

TERESA SELEE is a senior research scientist in the Sensors and Electromagnetic Applications Laboratory at GTRI. Her research interests include target tracking and target recognition of surface moving targets and ballistic missiles, as well as the effects of electronic attack and protection on tracking and discrimination efforts. Dr. Selee holds a B.A. in economics and a B.S. in mathematics from Youngstown State University as well as an M.S. in mathematics and a Ph.D. in applied mathematics from North Carolina State University.

JACQUELINE FAIRLEY is a research engineer in the Sensors and Electromagnetic Applications Laboratory at GTRI. Her research interests include development, testing, evaluation, and real-time implementation of radar signal processing algorithms and architectures. Dr. Fairley holds a B.S. in electrical engineering from the University of Missouri-Columbia, as well as an M.S. and Ph.D. in electrical and computer engineering from the Georgia Institute of Technology.

RYAN HERSEY is a principal research engineer and head of the Advanced Processing and Algorithms Branch at GTRI’s Sensors and Electromagnetic Applications Laboratory. He is the project director and principal investigator for multiple programs developing and implementing advanced intelligence, surveillance, and reconnaissance (ISR) systems. He specializes in adaptive array processing, simulation, and modeling and is highly experienced in the field of adaptive array processing, particularly in the application area of GMTI through space-time adaptive processing. Dr. Hersey holds a B.S. and M.S. in engineering science and mechanics from Penn State University and a Ph.D. in electrical and computer engineering from the Georgia Institute of Technology.

The MX/Peacekeeper and SICBM: A Search for

SURVIVABLE BASING

By Eugene Sevin

INTRODUCTION

During the mid-1960s, the aggressive efforts of the Soviet Union to expand its intercontinental ballistic missile (ICBM) force, improve its accuracy, and develop an effective anti-ballistic missile defense led to a re-evaluation of the survivability of the U.S. land-based nuclear forces. In late 1966, the Pentagon undertook a study called Strategic Experimental (or STRAT-X) to consider a range of possible future nuclear weapons. It was a national effort of great influence and led over time to the sea-based component of the nuclear triad, multi-warhead ICBMs, and increased hardness; it was the inspiration for both the MX Peacekeeper ICBM and the Trident submarine-launched ballistic missile [1].

The Air Force, under both the Carter and Reagan administrations, pursued development of a successor missile system to Minuteman III that would provide

Photo Credit: Nuclear Missile Silo.

Photo Source: Steve Jurvetson via Flickr Creative Commons.

increased range, variable warhead yields, improved accuracy, and improved survivability [2]. There were many discussions in the mid-1970s about whether the primary purpose of the MX program was to develop a new missile of highly improved accuracy and payload capability or whether the primary objective was to make the system more survivable. While it was generally agreed that both parts of this problem had to be solved, in almost everyone's mind, the primary objective of the MX program was to make a new generation of ICBMs more survivable. Because each of the basing modes under consideration was susceptible to some type of damaging nuclear weapon effect, the Defense Nuclear Agency (DNA) (now the Defense Threat Reduction Agency [DTRA]) played a central role in the Air Force's basing deliberations.

DNA'S PARTNERSHIP WITH THE AIR FORCE

Considering that survivability was primarily an issue of nuclear weapons effects, it was inevitable that DNA would play a significant role in the Air Force's basing deliberations. As it happened, the Air Force Ballistic Missile Office (BMO) looked to the agency to fund the requisite Nuclear Hardness and Survivability (NH&S) effort for each of the basing concepts on the basis that "that was DNA's business." The DNA Deputy Director for Science and Technology (DDST) at the time, the late Peter Haas, said he would be pleased to support the Air Force as long as it agreed to take DNA along with DNA's money.

So, DNA and BMO partnered for more than a decade to identify a survivable and acceptable basing mode for the

MX missile. As the particular nuclear weapon effect vulnerability for a basing concept was identified, DNA undertook necessary analyses and tests to gather data and determine the viability of the concept. For example, certain design considerations for the multiple protective system (MPS) were to ensure compatibility with strategic arms limitations (e.g., viewing ports in the tops of each shelter allowed Soviet national technical means to assure themselves that there was not a missile inside). The reason for such complications was that it was assumed at that time that the Soviets would never agree to on-site inspections.

Probably the three greatest contributions DNA made to the basing programs were (1) development and definition of the nuclear environments specific to each basing system, (2) proof-of-principal tests demonstrating crucial survivability conditions for the small ICBM (SICBM) based in hardened mobile launchers, and (3) development of superhard silo technology in combination with a fundamental reinterpretation of nuclear cratering data and high-shock-strength airblast propagation. The following sections discuss each of these contributions.

BASING ALTERNATIVES

The United States has considered many possible missile basing modes since the early 1960s, beginning with the STRAT-X study in 1966–67. Most fall into two categories: (1) free mobile systems in which missiles are moved on trains, trucks, aircraft, submarines, etc., over large areas (often hundreds of thousands of square miles) and are not tied to fixed shelters; and (2) multiple aim point (MAP) systems in which missiles are shuttled among

a large number of potential launch sites. Preliminary design was begun on such shelter systems, including (1) a continuous shallow-buried trench several miles in length, and (2) a MPS in which some number of missiles are randomly distributed among a much larger number of shelters.

In 1980, the Office of the Secretary of Defense (OSD) published a summary of 30 different missile basing concepts, identifying both positive and negative evaluation factors for each [3]. The concepts ranged from (1) no rebasing (launch under attack, orbital-based), (2) water-based (shallow underwater, inland ships, ocean ships, etc.), (3) aircraft-based (short takeoff and landing aircraft, vertical takeoff and landing aircraft, dirigible, etc.), and (4) land-based (proliferated, unsheltered, superhard, trench, MPS). The latter category contains 18 separate concepts including 5 separate MPS systems.

The survivability of the SICBM is achieved through a combination of hardness and mobility.

MAP Concepts

Covered Trench

The shallow buried trench (covered trench) basing envisaged the MX on a mobile launcher moving within a miles-long, near-surface-covered trench. The question arose as to whether it was possible for a nuclear fireball intersecting the trench to

cause the trench to act as a nuclear shock tube along its entire length. This concern gave rise to the HYBLA GOLD nuclear underground test to answer this question.

The HYBLA GOLD test was conceived, designed, and executed successfully in record time. The test bed consisted of five air-filled concrete shock tubes coupled to a single nuclear device. The primary objective was to obtain detailed measurements of high-enthalpy plasma behavior in these shock tubes; a secondary objective was the evaluation of instrumentation for such measurements [4].

Measurements were of three basic types: close-in pressure, pipe-wall pressure, and pipe-wall ablation. This event marked the first successful use of Manganin pressure gauges in the close-in nuclear environment. The steel flatpack pressure gauges met the design requirement of long recording times, which ranged from 800 ps to greater than 2.5 ms, with 38 of the 40 pipe-wall pressure gauges working properly at shot time. Pipe-wall pressures were substantially lower than pre-shot predictions; attenuation of plasma pressure with range along the shock tubes was higher than predicted. SRI International ablation gauges were a new concept designed for HYBLA GOLD. A total of 33 channels were fielded; 32 worked properly at shot time. In addition to providing data on pipe ablation depth vs. time, these gauges provided data on plasma conductivity and secondary low-resolution information on pipe pressure, pipe-wall strain, and pipe-wall temperature. Inferred ablation rates were orders of magnitude higher than pre-shot predictions.

It was concluded that natural attenuation mechanisms within the

trench likely would mitigate shock-tube-like effects on the missile to where conventional protective measures (e.g., blast plugs fore and aft of the missile) were practical.

Another potential vulnerability was progressive collapse of the tunnel from external airblast loading, a so-called “toothpaste tube” effect. These questions were never finally answered, as development of the trench concept was not pursued.

MPS Concepts

The evaluation of the MX/MPS basing concept identified no negative features. As adopted by the Carter administration, 200 MX missiles and launchers would be moved at random among 4,600 shelters in Nevada and Utah. The shelters are located about a mile apart and hardened to a level in which a direct hit on one will not disable another shelter or a hit between shelters would not damage two or more shelters. In concept, the shelter can be either horizontal or vertical. The vertical arrangement offers greater hardness at slightly lower cost; the horizontal geometry offers much more rapid relocation and allows for certain Strategic Arms Limitations Treaty (SALT) verification procedures. The shelters, some support facilities, and portions of two main operating bases are fenced and restricted from public use. The total restricted area occupies about 25–33 square miles. The remaining land is available to the public as before for grazing, agriculture, mining, recreation, etc. The total land area defined by the perimeter of the 200 clusters would have been approximately 8,000 square miles [5].

A number of high-explosive (HE) field tests were conducted to verify MPS shelter designs. The so-called SALT

viewing ports in the horizontal shelters were a major complication since they interfered with the structural continuity of the shelter and added to its complexity and cost. There were also lingering questions as to whether the SALT ports as implemented in the fielded design compromised the shelter’s design hardness.

When the Reagan administration came into office in 1981, it ordered a new look at the MX program and a re-evaluation of the decision to build the MPS system due to concerns ranging from preserving location uncertainty to outguessing the Soviet threat, as well as environmental impacts. President Reagan convened a blue-ribbon panel under the late Dr. Charles Townes to review once again all of the basing mode options. DNA served in a liaison role with the panel and briefed several alternative schemes involving superhard silo designs and deep underground basing. Dr. Townes recommended pursuing the design of a patterned configuration of superhard silos in a dense-packed array where fratricide acts to defeat the attack, as well as deep underground basing. Following the report of the Townes Panel, President Reagan cancelled the Carter MPS system. Preliminary design work continued on dense-packed and deep underground basing, but neither design concept reached a final design phase.

The second panel created by President Reagan was the President’s Commission on Strategic Forces, chaired by Brent Scowcroft [6]. Chairman Scowcroft undertook a substantially more expansive look at our strategic nuclear forces, essentially decoupling missile vulnerability from near-term MX/Peacekeeper deployment. He recommended that, as an interim measure, 100 MX missiles be deployed

in existing Minuteman silos and viewed as a modernization of the force, replacing the 100 Minuteman and the Titan II missiles being decommissioned. He also recommended that engineering design be initiated on a single-warhead ICBM, leading to full-scale development in 1987 and initial operating capability in the early 1990s, and that hardened silos or shelters and hardened mobile launchers be investigated as possible basing modes. In addition, he recommended that a program be undertaken to resolve the uncertainties regarding silo or shelter hardness, leading to later decisions about hardening MX in silos and deploying a small single-warhead ICBM in hardened silos or shelters. Finally, Chairman Scowcroft proposed that vigorous investigation proceed on different types of land-based vehicles and launchers, particularly including hardened vehicles. President Reagan fully endorsed the Scowcroft report in a letter to Congress [7].

The U.S. Congress was a major player in the MX program during both the Carter and Reagan administrations [8–11]. In the Defense Authorization Act of 1986, OSD was directed to “... conduct an independent review of the small missile and basing options conducted by the Defense Science Board.” A DSB Task Force was formed under Dr. John Deutch that reported out in October 1986. The Task Force concluded that “there is at least one SICBM basing mode—and possibly one or more MX basing modes—which, although costly, have a high degree of survivability and accordingly are suitable candidates for deployment by the U.S.” [12]. (See Caston et al. [13] for a somewhat more current review of basing options.)

The decision was made to deploy 50 Peacekeeper missiles in Minuteman III silos, and deployment began in 1986.

As a result of the Strategic Arms Reduction Treaty signed in 1991, the Peacekeeper force was deactivated. The deactivation was carried out beginning in 2003 and was completed in September 2005.

Closely Spaced (Dense-Packed) Basing

The potential for fratricide among attacking warheads if too closely spaced in both space and time has been known for some time. This fact was exploited as the fundamental concept of closely spaced (or dense-packed) basing. The concept was to build an array of superhard silos, spaced close enough together so that incoming warheads could not attack them all at the same time. Thus, between waves of an attack, the surviving missiles would launch out.

Superhardening of the silos was an essential aspect of the plan, which imposes fratricide-like conditions in an attack. Dr. Townes’ panel endorsed this concept, but indications are that he had second thoughts that he communicated privately to Secretary of Defense Casper Weinberger. In any event, Weinberger convened a special panel to critique the basing concept [14], which subsequently was discarded.

SUPERHARD SILOS

Hardening Potential

Although much was known about silo hardening, the systems development side of the defense community showed little interest in the subject during the Minuteman years except for the short-lived Hard Rock Silo program in the early 1970s. The apparent vulnerability of fixed silo-based ICBMs to threat projections of increasingly accurate, reliable, and numerous warheads prompted a search for survivability in

other directions (e.g., by combining hardness with mobility, deception, and defense).

Simulated nuclear blast tests of model silos during the 1970s showed heavily reinforced concrete structures to possess surprisingly great ductility and post-yield resistance when loaded impulsively. These results suggested that hardness levels substantially above anything previously contemplated might be achieved with conventional technology.

Research on high-shock-strength airblast had profound implications for structural hardening once it was recognized that early-time pressure impulse, rather than peak pressure, was the more appropriate damage indicator. With this stimulus, research in superhard construction soon led to radically improved designs. Detailed calculations indicated that overpressure waveforms at high shock strength decayed much more rapidly and, consequently, delivered a lesser total impulse to the silo during the first phase of loading than earlier thought.

Experimental confirmation of this fact was obtained by detonating a small nuclear device on the floor of a large, air-filled, underground chamber to simulate an atmospheric surface burst for a short period of time (Mini Jade underground test).

Blast tests of underground concrete structures showed the attenuation of ground shock in dry energy-dissipative soils (e.g., dry alluvium) to be much more significant at shallow depths of burial, decaying to half peak value in a fraction of the time originally thought. This effect contributed an order of magnitude increase in assessed structural hardness and emphasized

the importance of “beneficial siting.” Inasmuch as hard structures respond to a combination of peak pressure and impulse, this reduction in early-time impulse constituted an effective increase in assessed hardness.

Much of the work on superhardening was experimental in nature and was performed both by the Air Force Civil Engineering group of the Air Force Weapons Laboratory at Kirtland AFB in Albuquerque, NM, and the U.S. Army Corps of Engineers at the Waterways Experiment Station (WES) (now the Engineer Research and Development Center [ERDC]) at Vicksburg, MS [15, 16].

Consequently, superhardening—a 50- to 100-fold increase in hardness over Minuteman silos—was viewed as a competitive strategy to thwart the effectiveness of Soviet ICBM modernization plans. Critics of superhardening invoked a chess game analogy where regardless of target hardness achieved, Russian accuracy improvements would lead to checkmate. Proponents countered with

a “Game of Chicken” analogy wherein superhardness would challenge them on major new technology investment, undesirable force structure (especially in view of arms control limits), and operational difficulties while retaining substantial targeting uncertainties. In the end, however, the accuracy argument beat out hardening.

Figure 1 shows scale models of the silo headworks being positioned for an explosive test at ERDC’s Fort Polk, LA, facility. A launch tube model is shown being emplaced in Figure 2. An artist’s conception of a superhard silo is shown in Figure 3.

Cratering Effects

The size of a nuclear crater and associated ground motions also pose significant design challenges for superhardening. Theoretical predictions of crater formation did not agree with the HE data and the few large-yield nuclear tests in the Pacific. Theory has consistently indicated much smaller craters and ground motions, as well as

a strong dependency of crater size on geology.

The Mini Jade “atmospheric” chamber test mentioned previously not only provided critical airblast data but also demonstrated a new capability for cratering experimentation. The chamber remained intact post-test, and measurements of the crater were in good agreement with analytical predictions. A subsequent chamber experiment (the Mill Yard underground test) was conducted with a different near-surface geology, and extensive ground motion measurements were obtained; these results also supported the analytical model. These findings motivated a two-year geophysical exploration of selected nuclear craters at the Pacific Proving Grounds (PPG) (the Pacific Enewetak Atoll Crater Exploration [PEACE] program) conducted by the U.S. Geological Survey, which has brought the empirical basis for yield scaling in line with theoretical expectations.



Figure 1: Models of Silo Headworks Being Readied for Test.



Figure 2: Launch Tube Being Emplaced for Test.

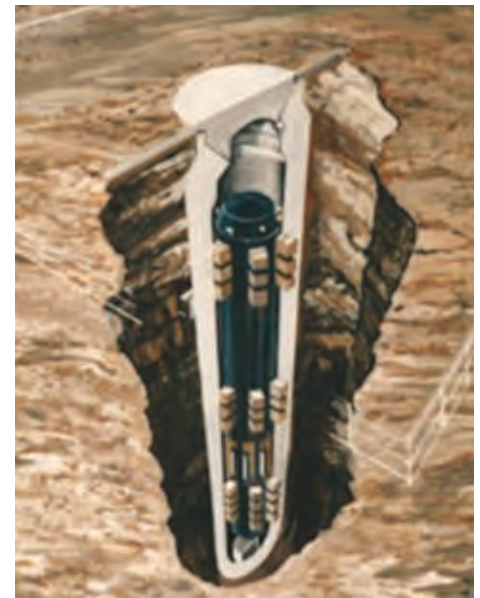


Figure 3: Artist's Conception of Superhard Silo.

The PEACE Program

Peace Program Background

The two-year PEACE program was performed by the U.S. Geological Survey for DNA in 1984/85. It involved stratigraphic analysis and other geologic and geophysical studies in the vicinity of OAK and KOA craters and included underwater explorations [17].

The only experimental cratering data for strategic-scale, near-surface nuclear bursts are from the PPG tests, fired on or near coral atolls. Earlier interpretation of these data—based largely on photography, surface surveys, and lead-line measurements—gave these craters broad, saucer-shaped profiles (large aspect ratios) and large volumes. Extrapolated to continental geologies with the aid of calibration tests performed using HE, these data became the basis for the crater volumes in earlier editions of DNA's authoritative Effects Manual-1 (EM-1).

These crater dimensions were much larger than those calculated in DNA's Benchmark Cratering Program using first principles physical models in large computer codes (collectively referred to as BM-3); these acquired a high level of credibility as a result of extensive peer review. Portions of the models were also validated by comparison with data from underground nuclear tests and HE simulation tests.

Based partly on certain features of the OAK crater observed during earlier programs, the belief grew that the large volumes and aspect ratios of the PPG craters were due to geologic factors that were unlikely to be important to continental basing or targeting. The PEACE program was undertaken by DNA to more thoroughly characterize these craters, to provide a quantitative basis

for understanding their development, and to determine the relevance of the PPG craters to strategic basing and targeting issues.

Figure 4 shows a comparison of the old EM-1 crater profiles for a 6-MT contact burst on dry soil over wet soil geology. Overpressures of 30,000 psi occur at the edge of the crater specified by the old EM-1; the same overpressures occur at more than twice the radius of the crater calculated by the BM-3 methodology.

The craters chosen for exploration during PEACE were OAK and KOA. The OAK crater resulted from a 9-Mt device fired on a barge anchored in 15 ft of water in the lagoon adjacent to the atoll island. Interpretation of both OAK and KOA is complicated by geological asymmetry (i.e., atoll reef on one side, lagoon on the other). The effect of the barge on source coupling further complicates OAK. The KOA crater resulted from a 1.4-Mt device fired on an atoll island. The KOA device was surrounded by a water tank, providing approximately 3 m of water tamping. This simplifies the modeling of source coupling physics; however, interpretation of the KOA crater is

additionally complicated by the fact that several other large-yield devices had been previously fired close enough to KOA ground zero to have altered the properties of the coral in that region.

Despite the factor-of-six difference in yields, the apparent dimensions and profiles attributed to the OAK and KOA craters are similar, indicating that the energies that went into forming the craters in these events were about the same. This longstanding observation bears strongly on the rationale for developing weapons with enhanced coupling, such as shallow earth penetrators.

Conflicting Hypotheses

During the planning for PEACE, there were two principal and conflicting hypotheses to explain the large apparent volume and aspect ratios of OAK and KOA: (1) a small bowl-shaped, early-time crater, and (2) a large bowl-shaped, early-time crater.

Small Bowl-Shaped, Early-Time Crater. In this hypothesis, the volume of the early-time crater was much smaller than the volume of the saucer-shaped apparent crater. The shape change (from bowl to saucer) was due

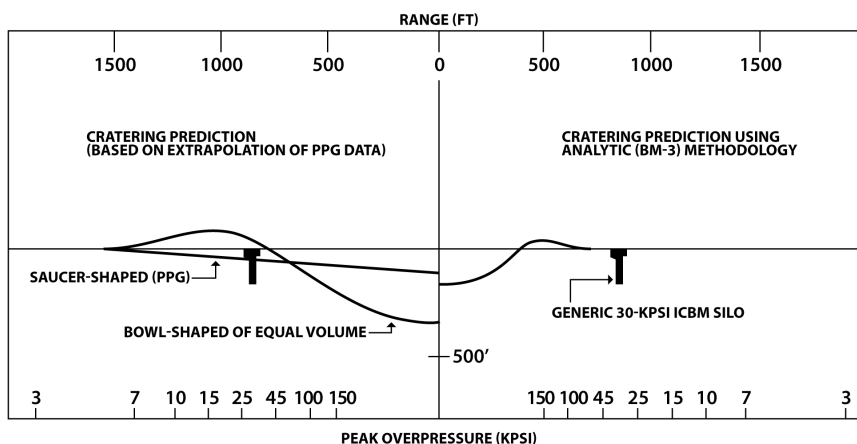


Figure 4: Comparison of Old EM-1 and Theoretical (BM-3) Crater Dimensions.

to slumping of the transient crater walls and to subsidence of the surrounding wings (as illustrated in Figure 5).

A large increase in volume was associated with such post-event subsidence, which was presumed to have occurred under a large area of the sea floor. This subsidence was due to densification of the underlying coral, brought on by fracture of the weak, frangible skeletal structure of the highly porous coral. The hypothesis of a small early-time crater would indicate that energy coupling from contact bursts is inefficient, which is consistent with the BM-3 prediction methodology.

> Large Bowl-Shaped, Early-Time Crater. In this hypothesis, the volume of the early crater was comparable to the volume of the final apparent crater. The shape change was due to slumping of the crater walls and to converging flow of the surrounding region (a constant-volume process), as illustrated in Figure 6.

The large volume of the early-time crater was due either to more efficient source coupling than has been calculated by the BM-3 models or to weakness of the medium (e.g., due to transient liquefaction), which could lead to nearly hydrodynamic behavior during the formation of the crater.

Key Observations

> Small Inner Craters. The sea floor profiles for both OAK and KOA consist of small central craters with distinct edges, surrounded by a depressed wing extending to the apparent radii. Abundant evidence of these small central craters was obtained from direct observations (scuba and research submarine surveys) and bathymetry, as well as from seismic surveys, downhole logging, and analysis of borehole samples.

> Similarities of OAK and KOA. The OAK-KOA similarities extend to the small central craters, the crater floor, and the “zone of sonic degradation,” though the craters differ in some of their subsurface geologic horizons. In terms of these effects, the energies coupled into ground motions from OAK (9 Mt on a barge) and KOA (1.4 Mt in a water tank) were about the same. This finding is important to theoretical results that indicate greatly enhanced energy coupling for shallow earth-penetrating weapons relative to contact bursts.

The depth of burst (DOB) equivalence of KOA can be estimated on the basis of the depth of water above and surrounding the device (3 m) or its equivalent mass of soil (1.5 m). Thus,

KOA was at the equivalent of somewhat less than $1.4 \text{ m/Mt}^{1/3}$ scaled DOB; horizontal confinement in the KOA tank was less than that which occurs in an actual DOB geometry.

> Long-Term Subsidence. An important discovery during the Marine Phase was the existence of a line of vertical steel rails on the depressed wing of KOA (i.e., within the apparent crater radius). These same rails appear on pretest drawings and photos as periodic supports for a long retaining wall that extended toward the KOA water tank. Today, they are still embedded in the beach rock, but they are under varying depths of water, extending inward to the edge of the small central crater. Another important marker (also seen in earlier surveys) is a concrete framework used to support one of the experiments at 1,830 ft from KOA. This frame was photographed before the event, a few days afterward, several months afterward, and again during PEACE. Before the test, it was a few feet above sea level, but its elevation in 1984 was several feet below sea level, with little or no horizontal displacement.

These rails and the concrete frame serve as Lagrangian markers showing late-time vertical subsidence on the wings of the crater. Further, comparison of bathymetric surveys made in 1958 (D + 58 days) and in 1984 show that the OAK crater floor dropped 20 to 40 ft in the central region and 5 to 10 ft on the surrounding wings between 1958 and 1984. Thus, 25 to 30% of 1984’s apparent crater volume in coral formed more than 2 months after the event. An appreciable but unmeasurable fraction of the apparent crater probably formed in the interval between a few minutes after the event and D + 58 days.

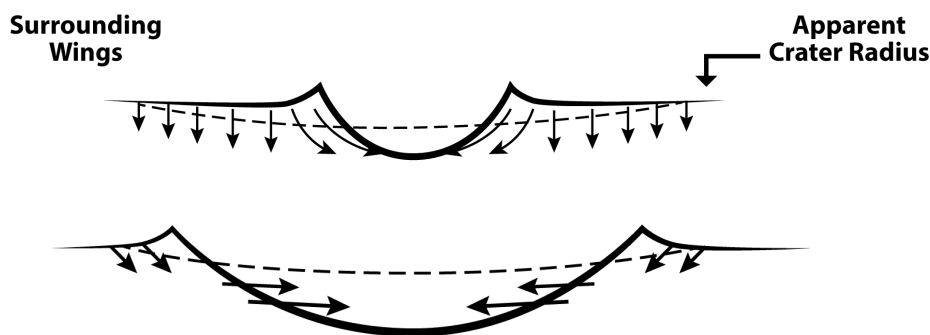


Figure 5 (top): Small Bowl-Shaped, Early-Time Crater.

Figure 6 (bottom): Large Bowl-Shaped, Early-Time Crater.

Peace Program Conclusions

The existence of the small inner craters affirmed the early-part of the small crater hypothesis that energy coupling from contact bursts of radiative sources is highly inefficient, as predicted by BM-3. The small central craters resulted from early-time excavation and flow processes. Soon thereafter, the unstable walls collapsed, or slumped, out to the presently observed central crater radii. Within these radii, strategic structures would experience severely disruptive environments involving large horizontal and vertical distortions and gradients. Outside of these radii, the distortional environments are much less severe, arising perhaps from flows, and in part from slower subsidence processes in saturated coral sand. This slow subsidence would not be present in dry alluvium.

Superhardening—a 50- to 100-fold increase in hardness over Minuteman silos—was viewed as a competitive strategy to thwart the effectiveness of Soviet ICBM modernization plans.

The similarities of the OAK and KOA craters make it likely that the effective coupled energy from these bursts was essentially the same. Coupling from KOA was relatively uncomplicated,

due to the tamping effect of the larger water mass surrounding the source. We therefore can be fairly confident of calculations showing that approximately 2.7% of the energy from KOA was effectively coupled into kinetic energy of downward-moving material.

CRATERING GROUND MOTION SIMULATOR

The nuclear chamber test is not suitable for testing silos, and HE cannot achieve nuclear source region pressures. The simulation approach adopted for large-scale testing is a sequential, three-stage process, incorporating crater and airblast effects. Termed the Crater and Related Effects Simulator (CARES), and illustrated schematically in Figure 7, this simulation consists of an HE subsurface charge that replicates the calculated

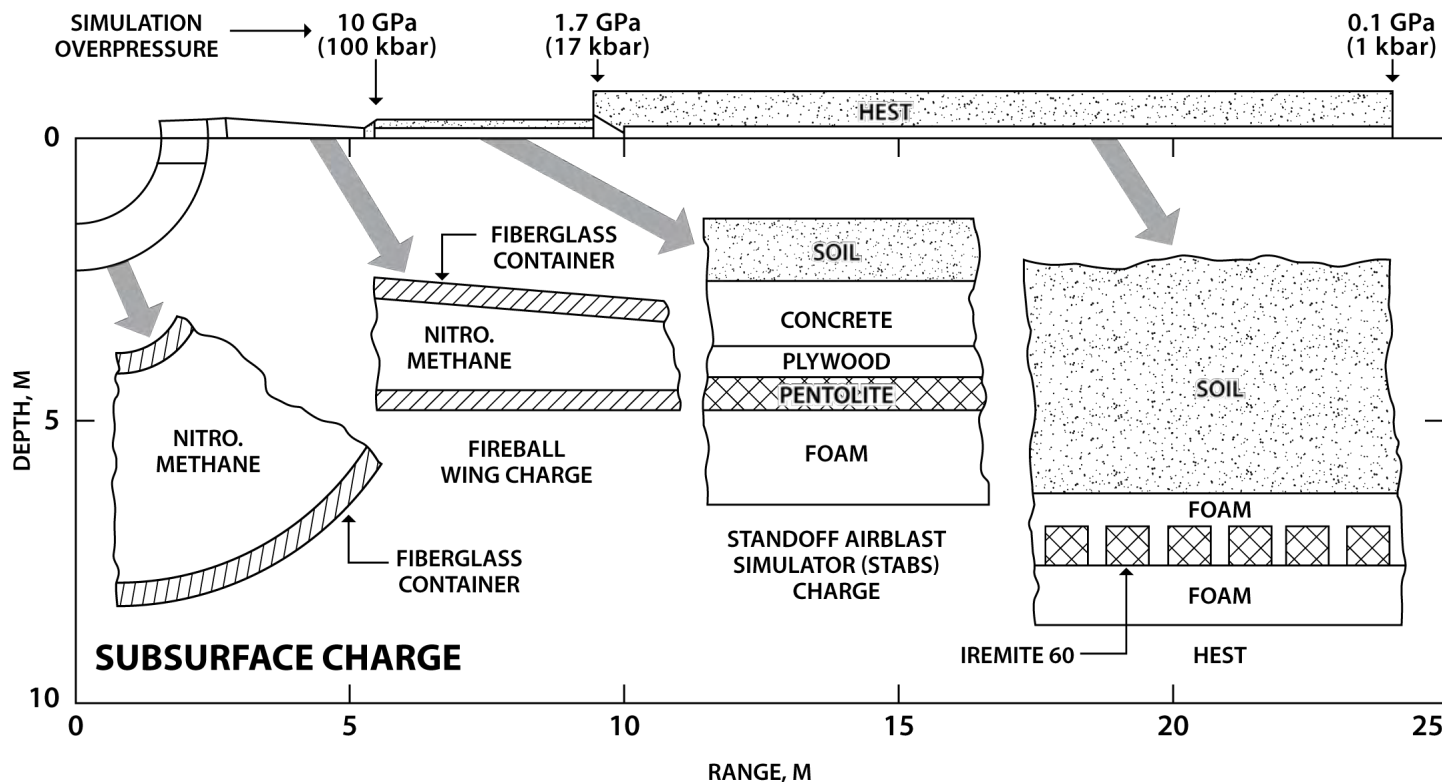


Figure 7: Cross-Sectional View of CARES.

pressure-velocity state at about the 50-kbar stage of the evolving nuclear crater, where subsequent pressures can be obtained with HE. (At this time, the crater has grown to about 5% of its final volume in a dry geology.) A sequentially detonated surface charge is used to simulate the airblast-coupled ground shock, transitioning into a conventional high-explosive simulation technique (HEST) bed to provide the primary airblast loading on the silo structure. Finally, in Stage 3, the ground motions measured in the CARES experiment is scaled up and reproduced in a large-size HEST-DIHEST (direct-induced HEST) configuration to provide a test bed for prototype silo structures.

With reference to Figure 7, the first stage is represented by the underground “atmospheric” test, where agreement between predictions and observations of ground motion and final crater dimensions is *presumed* to substantiate the early-time, hydrodynamic phase of the theory. Stage 2 consists of an HE simulation of the crater, close-in ground motions, and airblast. Practical considerations limit this to kiloton-yield equivalence [18].



Figure 8: CARES HE Simulator in Dry Alluvium at Yuma, AZ, Test Site (June 1985).

A fully instrumented CARES test replicating a 2-kt surface burst (1/8th scale for 1 Mt) provided the experimental rationale for establishing silo ground motion design criteria and designing large-scale HEST beds for silo validation testing. Figure 8 shows the CARES test bed under construction. Subsequently, a large-scale HEST test was conducted on a superhard silo that was full size for the SICBM or 5/8th-size for the Peacekeeper missile in which both airblast and direct ground motion effects were simulated.

THE HARDENED MOBILE LAUNCHER

Overview

The survivability of the SICBM is achieved through a combination of hardness and mobility. The idea of hardening the mobile launcher against a massive barrage attack was born out of a desire to reduce the land area needed for its deployment. A hardness level of several tens of pounds/square inch of overpressure can reduce the deployment area significantly over that

of an unhardened vehicle, and makes practical its deployment on selected military bases. Figure 9 shows the dependence of the number of attacking weapons needed to saturate the Hard Mobile Launcher (HML) deployment area for various levels of HML hardening. Hardening to levels of, say, 30 psi is no easy task, and it was fully appreciated from the outset that a radical vehicle design was required.

The HML is hardened structurally against direct airblast effects. Sliding and overturning blast forces are reduced by aerodynamic streamlining of the vehicle and by exploiting the stabilizing effects of the vertical airblast forces. This concept is brand new and requires that the vehicle be deployed intimately with the ground so that no equilibrating airblast pressure acts on the underside of the vehicle. This innovation was radical, doing away with external restraints or tie-downs for the vehicle. While substantially simplifying the design, the change clearly demands a detailed understanding of the airblast flow field, including time phasing of the vertical and horizontal airblast

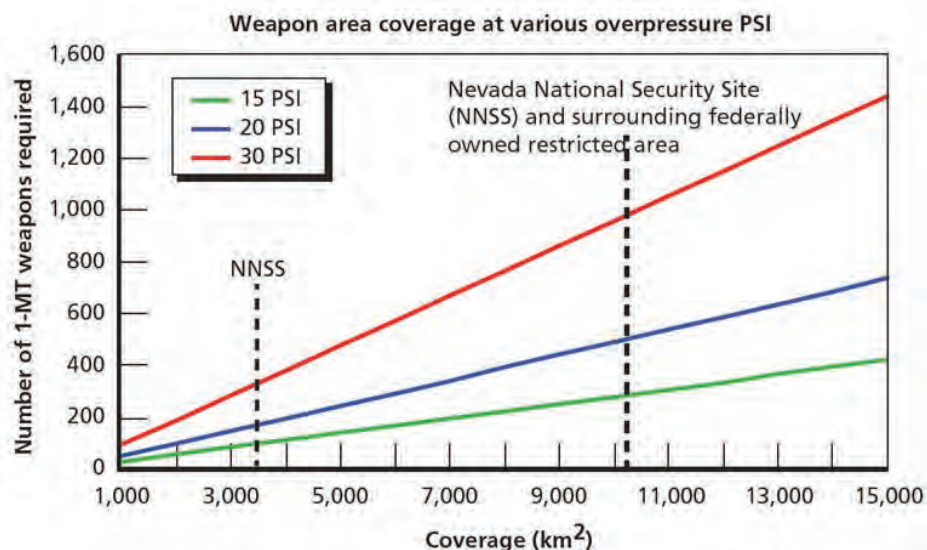


Figure 9: Impact of Hardness on HML Deployment Area [13].

components. A proof-of-principle experiment was conducted successfully in the Minor Scale HE field test. Figure 10 shows the functional modes of HML deployment.

The Air Force constructed two full-scale mobility test vehicles, one with wheels and one with tracks for mobility testing. Once a wheeled configuration was selected, mobility test and demonstrations were conducted with an engineering prototype vehicle, the Engineering Test Unit (ETU) [19, 20]. Figure 11 shows the HML ETU.

Airblast Loading and Precursor Simulation

It is known from atmospheric testing experience that nuclear airblast waveforms and flow fields along the ground are dependent on the weapon’s height of burst (HOB) and thermal properties of the ground surface. The radiating fireball heats the ground ahead of the advancing shock wave, causing it to propagate more rapidly along the surface than in the (cooler) air above. This effect leads to radical changes in the airblast shock structure and, by entraining surface materials into the flow, vastly increases the aerodynamic drag forces on above-ground objects. There is direct evidence from prior atmospheric nuclear tests that these so-called thermally precursed flow effects can have a dramatic influence on the response of “drag-type” targets such as ground vehicles. (See Frankel et al. [21] for a useful summary of a broad range of nuclear weapons effects, including uncertainties.)

Numerical simulations of complex flows have matured substantially in recent years. Examples of these state-of-the-art capabilities are shown in Figures 12 and 13 (which are courtesy

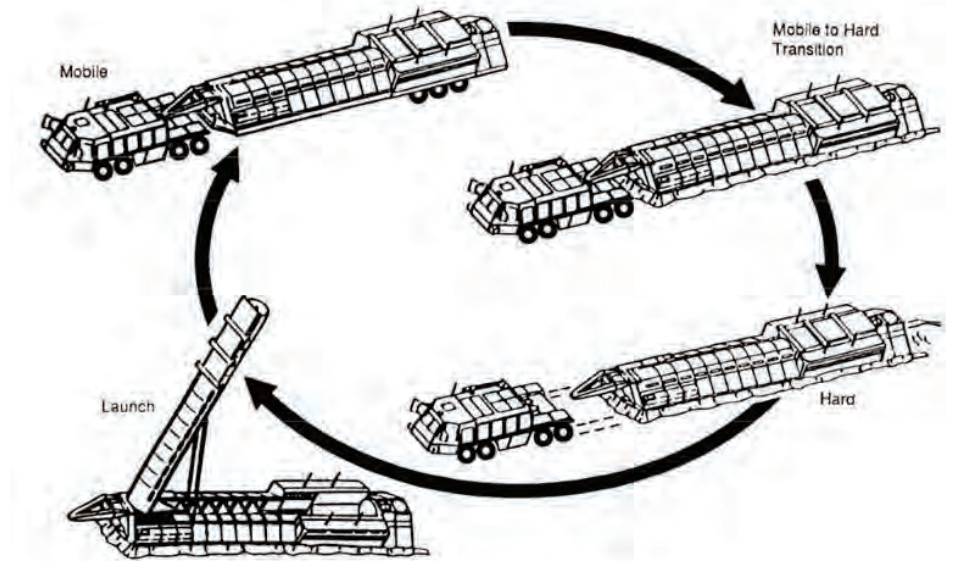


Figure 10: Functional Stages of HML/SICBM Deployment.



Figure 11: HML ETU.

of Messrs. Allen Kuhl from the Lawrence Livermore National Laboratory [LLNL] and John Bell from the Lawrence Berkeley National Laboratory [LBNL]). The top row of images in Figure 12 is a numerical simulation of blast wave reflection from surfaces showing turbulent mixing in explosions over different surfaces. Directly below each image is a shadowgraph showing the respective shock structure from shock tube experiments [22]. Figure 13 shows

the precursor shock structure and flow field from Operation Plumbbob, Priscilla Event (37-kt, 210-m HOB on 24 June 1958) using LLNL’s Adaptive Mesh Refinement (AMR) code [23].

DNA developed a novel method to simulate thermally precursed flow in the absence of a suitable thermal source. The underlying premise is that the flow develops as a consequence of the air shock propagating along the ground

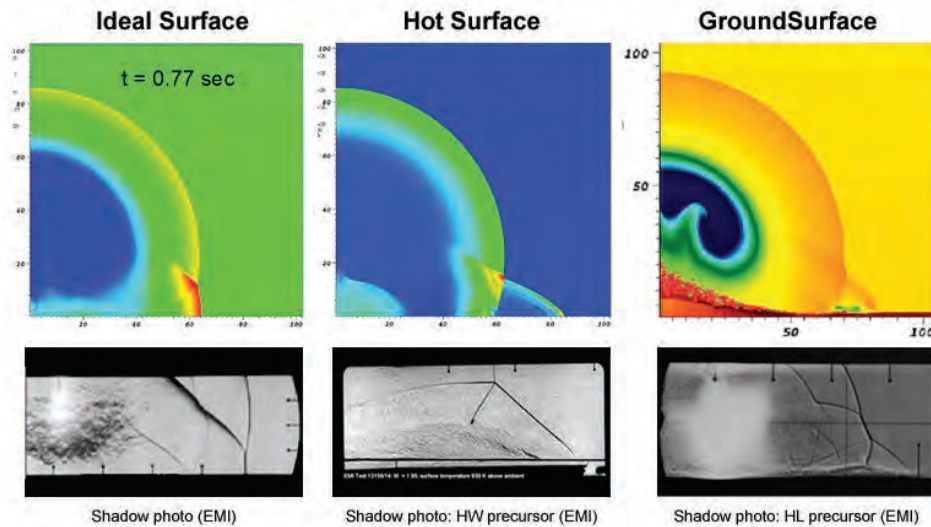


Figure 12: Turbulent Mixing in Explosions.

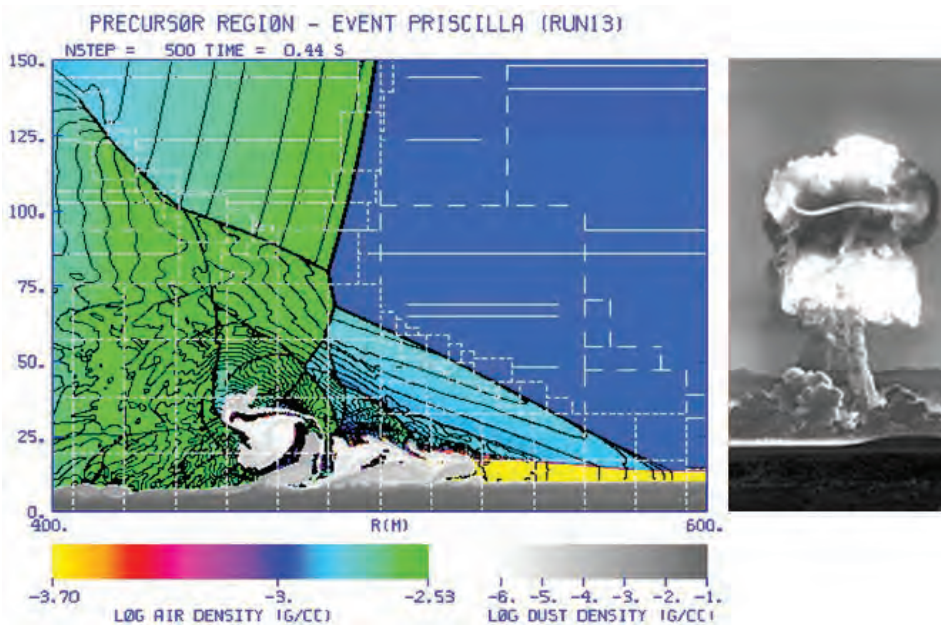


Figure 13: Precursor Shock Structure, Operation Plumbbob, Event Priscilla.

ahead of the main shock. While this effect is triggered in a nuclear burst by fireball preheating of the ground, it is not primarily a thermally dominated effect. Thus, it should be possible to replicate the flow in a layered, two-gas system of appropriately different sound speeds. This effect was accomplished at large scale under field conditions by confining a layer of helium gas along the

ground under a thin Mylar membrane. The speed of propagation is controlled by the concentration of helium, which, in turn, is related to nuclear yield and HOB through theoretically based estimates of surface air temperature.

This approach was investigated by means of extensive numerical simulations and comparison with

atmospheric nuclear data. It was tested in laboratory shock tubes at miniature scale and demonstrated successfully in HE field tests. Figure 14 shows the test setup in the Misty Picture event, an 8-kt nuclear equivalent HE source. A 0.5-mil-thick membrane measuring 400 ft wide x 900 ft long x 2 ft high contained helium at 95% concentration.

A test technique was qualified for hardness validation testing on this basis. One-fifth geometric scale models of two competing HML designs were tested in the Minor Scale event. This test was considered to be a successful proof-of-principle test for the HML design concept. Development of the SICBM and HML was terminated during the second Reagan administration, mostly for reasons of affordability.

THE FUTURE OF ICBM MODERNIZATION

Despite the remarkable technical achievements recounted herein, their impact on the U.S. nuclear posture has been essentially nil. In accordance with the Nuclear Posture Review (NPR) of April 2010, the Minuteman III Life Extension Program will continue with the aim of keeping the fleet in service to 2030, as mandated by Congress. The NPR notes that although a decision on any follow-on ICBM is not needed for several years, studies to inform that decision are needed now. Accordingly, the Air Force has completed an analysis of alternative deployment options, with the objective of defining a cost-effective approach that supports continued reductions in U.S. nuclear weapons while promoting stable deterrence.

This analysis of alternatives focuses on three options: (1) a “baseline” option that would extend the life of the Minuteman III through 2075, (2)



Figure 14: Misty Picture Test Bed Showing HE Source (in Background) and Mylar Helium Bag.

a “replacement system “capitalizing on the existing Minuteman III silo infrastructure, and (3) a “hybrid” option that would mix the existing Minuteman III silo infrastructure with new road-mobile ICBMs.

To be sure, the Air Force also is modernizing the Minuteman missiles, replacing and upgrading their rocket motors, guidance systems, and other components so that they can remain in the force through 2030. The Air Force plans to replace the missiles with a new Ground-Based Strategic Deterrent (GBSD) around 2030 [24]. The Air Force released a request for proposals for the GBSD system at the end of July 2016 [25].

Meanwhile, the U.S. land-based ballistic missile force will consist of 440 Minuteman III ICBMs, each deployed with one warhead in existing Minuteman III silos. The Air Force has concluded that incremental

modernization and sustainment of the current Minuteman III force is a cost-effective alternative to its replacement. Moreover, silo basing will likely continue to be the preferred option for the foreseeable future as the vulnerability of the Minuteman silos to a Russian preemptive strike is not nearly as much concern as it was during the Cold War [26]. That the “concern” and not the “vulnerability” is now reduced marks a major change in threat assessment and is the primary rationale for retaining silo basing.

In other words, the GBSD can be thought of as a “nuclear sponge” on a hair-trigger that would require some 500 attacking reentry vehicles (RVs) (or perhaps 1,000 from a reliability perspective) to successfully defeat in a preemptive strike. While a steep commitment of resources, the HML or covered trench would pose even a greater challenge to a potential attacker.

In conclusion, the problem of missile vulnerability has been defined away, not solved. As discussed by a report by the Defense Science Board [12] and Caston et al. [13], survivable basing solutions exist for both Peacekeeper and SICBM missiles, but their cost is probably two to three times the Minuteman upgrade cost. Clearly, a careful threat analysis is required as part of the GBSD design effort. It is further recommended that consideration of mobile basing take full advantage of the technology recounted in this article, including both the hardened mobile launcher and the covered trench. ■

REFERENCES

- [1] Grier, Peter. “STRAT-X.” *Air Force Magazine*, January 2010.
- [2] Medalia, Jonathan E. “Assessing the Options for Preserving ICBM Survivability.” Report No. 81-222F, 28 September 1981.

[3] Office of the Deputy Under Secretary of Defense for Research and Engineering (Strategic and Space Systems). "ICBM Basing Options: A Summary of Major Studies to Define a Survivable Basing Concept for ICBM." December 1980.

[4] DeCarli, Paul S. "HUSSAR SWORD Series, HYBLA GOLD Event: Stress and Ablation Measurements." POR 6973, SRI International, 1 February 1979.

[5] Office of Technology Assessment. *MX Missile Basing*. September 1981.

[6] President's Commission on Strategic Forces (Scowcroft Report). "Report of the President's Commission on Strategic Forces." 6 April 1983.

[7] Reagan, Ronald. "Letter to Members of the House of Representatives on Production of the MX Missile." 19 July 1983.

[8] U.S. General Accounting Office. "The MX Weapon System: Issues and Challenges." Comptroller General Report to the Congress of the United States. 17 February 1981.

[9] Medalia, Jonathan E. "The MX Basing Debate: The Reagan Plan and Alternatives." Issue Brief Number 1B81165, Library of Congress Congressional Research Service, 2 November 1981.

[10] U.S. General Accounting Office. "Small ICBM." Report NSIAD-91-275, 30 September 1991.

[11] Medalia, Jonathan E. "MX Intercontinental Ballistic Missile Program." Issue Brief Number IB77060, Library of Congress Congressional Research Service, Updated 14 December 1981.

[12] Office of the Under Secretary of Defense for Research and Engineering. "Small Intercontinental Ballistic Missile Modernization." Defense Science Board Task Force Report, Washington, DC, March 1986.

[13] Caston, Lauren, et al. "The Future of the U.S. Intercontinental Ballistic Missile Force." RAND Project Air Force, 2014.

[14] Pincus, Walter. "Weinberger Sets Up Panel to Criticize MX Missile Dense Basing." *Washington Post*, 20 June 20 1982.

[15] Sevin, Eugene. "Validation Testing of Nuclear Survivable Systems." 59th Shock and Vibration Symposium, Albuquerque, NM, 18 October 1988.

[16] Sevin, Eugene. "Superhard Facilities: Design & Test Concepts." Defense Nuclear Agency, Washington, DC, 1985.

[17] Henry, Thomas W., and Bruce R. Wardlaw. "Enewetak Atoll and the PEACE Program: Geological and Geophysical Investigation of Enewetak Atoll, Republic of the Marshall Islands." U.S. Geological Survey Professional Paper 1513-A, 1990.

[18] Cowler, M. S., et al. "DRY CARES Pre-Test Calculation of Cratering and Ground Motion." DNA-TR-85-208, Defense Nuclear Agency, May 1985.

[19] ICBM Hard Mobile Launcher. <https://www.youtube.com/watch?v=T8OV5rbfZ6o>, 9 January 2014.

[20] VirtualGlobetrotting. "Small ICBM Hard Mobile Launcher, Dayton, Ohio (OH)." <http://virtualglobetrotting.com/map/small-icbm-hard-mobile-launcher/view/google/>, 16 August 2007.

[21] Frankel, M., J. Scouras, and G. Ullrich. "The Uncertain Consequences of Nuclear Weapons Use." The Johns Hopkins University Applied Physics Laboratory, 2015.

[22] Kuhl, A. L. "Validation of Numerical Simulations of Explosion Fields." LLNL-TR-609492, Lawrence Livermore National Laboratory, 2013.

[23] Kuhl, A. L. "Turbulent Wall Jet in a Blast Wave Precursor." *1993 Japanese National Symposium on Shock Wave Phenomena*, edited by K. Takayama, Tohoku Print, Sendai, Japan (also published as UCRLJC-112713), 1994.

[24] Woolf, Amy F. "U.S. Strategic Nuclear Forces: Background, Developments, and Issues." Congressional

Research Service, Report 7-5700, 10 March 2016.

[25] Insinna, Valerie. "Air Force Kicks Off Competitions for Two Critical Nuclear Programs." *Defense News*, 29 July 2016.

[26] Caston, Lauren, et al. "The Future of the Intercontinental Ballistic Missile Force." RAND Project Air Force Report, 2011.

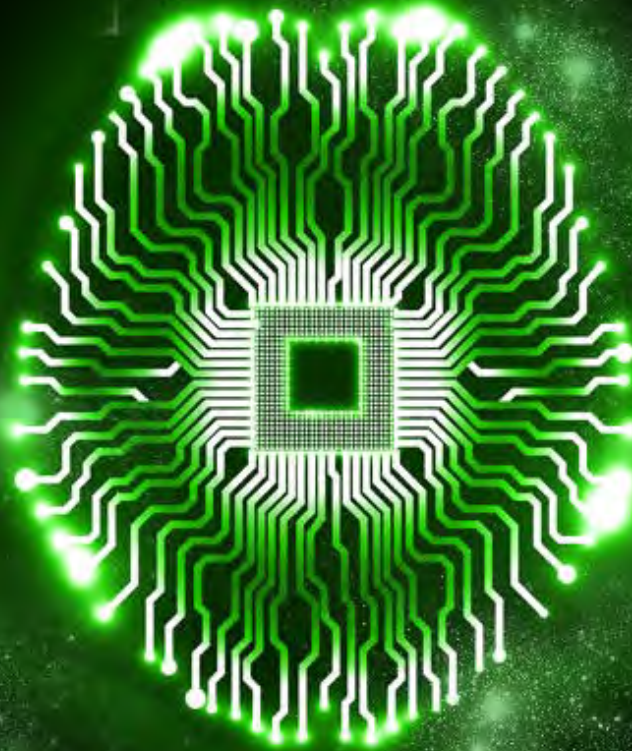
ACKNOWLEDGMENTS

The author acknowledges the following colleagues for reviewing drafts and providing helpful suggestions for this article: Dr. Dan Burgess, Dr. Richard Cramond, Mr. Ken Kreyenhagen, Dr. Byron Ristvet, Dr. Jeff Thomsen, and Dr. George Ullrich. The author is also indebted to Dr. Reed Mosher and his staff for locating the superhard silo test photos in their archives. Finally, the author thanks the many distinguished engineers, scientists, and managers at the Air Force Ballistic Missiles Office, their supporting contractors, and supporting government laboratories.

BIOGRAPHY

EUGENE SEVIN is an independent consultant with expertise in nuclear and conventional weapons effects, hardened facility design, and computational structural mechanics. He has provided consulting services to Engility Corporation, the Defense Threat Reduction Agency, the Institute for Defense Analyses, and others. In addition, his government service includes serving as DNA's Chief of the Strategic Structures Division, DNA's Assistant to the Deputy Director (Science and Technology) for Experimental Research, and Director of Space and Missiles Systems for the Office of the Secretary of Defense. Dr. Sevin has also held numerous academic positions, including Adjunct Professor of Applied Mechanics at Illinois Institute of Technology (IIT), Director of Engineering Mechanics Research at IIT's Research Institute, Professor of Mechanical Engineering at the Technion (Israel Institute of Technology), and Head of Mechanical Engineering at Ben Gurion University of the Negev. He holds a Ph.D. in applied mechanics and a B.S. in mechanical engineering from the Illinois Institute of Technology, as well as an M.S. in mechanical engineering from the California Institute of Technology.

Real-Time,
In Situ Intelligent
Video Analytics:
Harnessing the
Power of GPUs for



DEEP LEARNING APPLICATIONS

By Shawn Recker and Christiaan Gribble

A DATA EXPLOSION

From the edges of the observable universe to medical image scanners on Earth, there is an ever-growing need to quickly process and understand large amounts of audio and visual data. Audio data capture a wide range of frequencies, for example; and human speech patterns are incredibly complex and extremely diverse. Similarly, visual data come in many forms, including video sequences, images from multiple cameras, medical scanners, etc. And recent trends with

big data have produced large quantities of labeled data from which interesting patterns have yet to be discerned and used. Not surprisingly, processing such data in situ at interactive rates without significant hardware requirements is one major challenge arising from the big data revolution.

Applications in a variety of domains require accurate and robust processing of these types of data to achieve specific goals. One of the most common problems is image recognition, in which a solver must identify main

objects of interest in image data. The demand for faster and more accurate image recognition algorithms has led to the development of several image recognition databases and contests, of which the ImageNet Large Scale Visual Recognition Challenge (ILSVRC) is the most well-known [1].

Figure 1 shows accuracy trends for ILSVRC contest winners over the past several years. Whereas traditional image recognition approaches employ hand-crafted computer vision classifiers trained on a number of instances

of each object class, in 2012 Alex Krizhevsky entered a deep neural network (DNN), now known as AlexNet, that reduced the error rate of the next closest solution by more than 10% [2]. By 2015, the winning ILSVRC algorithm rivaled human capabilities, and today deep learning algorithms exceed human capabilities.

The success of AlexNet is regarded by many as the genesis of deep learning's resurgence [3]. While notionally deep learning has existed in various forms since the early 1980s, only recently have deep learning algorithms become computationally practical. Modern graphics processing unit (GPU) architectures, now explicitly designed for deep learning algorithms, have enabled many of the recent and impressive achievements of contemporary deep learning techniques.

At the same time, these massively parallel architectures are driving the next generation of deep learning algorithms for intelligent video analytics (IVA). IVA broadly categorizes events, attributes, or patterns of behavior in video data. For example, automatic target recognition (ATR) defines the process of identifying and localizing an object in an image (e.g., a person in the top-left corner of the image). ATR capabilities also extend to event detection (such as isolating a person running) and path analysis (such as determining how people cross a busy intersection). These capabilities combine to create systems capable of providing intelligent, actionable insights to human users.

One system that is being built to leverage many of these advancements is Sentinel™. Developed by the SURVICE Engineering Company in Belcamp, MD, this system (which is discussed in detail later) combines state-of-the-

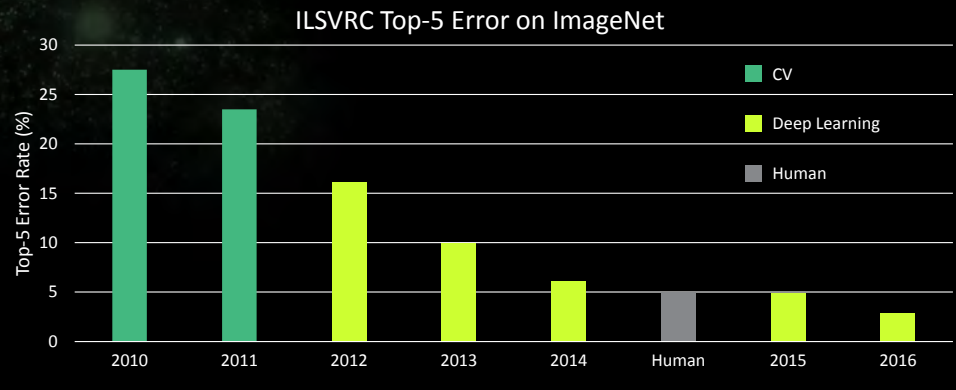


Figure 1: ImageNet Top-5 Classification Error Over Time.

art techniques in high-performance computing (HPC), modern data reduction and analysis techniques, and deep learning to realize ATR, tracking, event detection, and other visually oriented tasks. These components combine to create a flexible, scalable system for improved situational awareness in a variety of intelligence, surveillance, and reconnaissance (ISR) scenarios.

DEEP LEARNING

The possible applications of modern deep learning are both wide and deep. Recently, deep learning has been applied successfully to problems in representation learning. For example, a variety of factors influence every single piece of data in many real-world classification problems: a picture of a red car in broad daylight will contain red pixels, whereas a picture of that same car at night will exhibit nearly black pixels. Deep learning solves the representation learning problem by building complex representations (wheels or headlights) from simpler concepts (edges, color, and so forth) [4].

One common example of a deep learning model is the feedforward DNN. Originally inspired by biological neuron models, this DNN is composed of artificial neurons, which take some number of inputs and produce a single

output. Perhaps the first artificial neuron was the perceptron [5], which produced a simple binary output from simple binary inputs. Modern neurons are often modeled on sigmoid functions, which produce an output in the range [0,1] given inputs in the same range. Neurons combine to form a network comprising (possibly) several layers, where each layer has some number of neurons and each neuron is fully connected to the subsequent layer.

Figure 2 illustrates a typical DNN. On the left side of the figure is an example artificial neuron, which takes some number of inputs to produce a single output. There exist many types of artificial neurons, but the most common are compute sigmoid, linear rectified, or hyperbolic tangent functions. On the right side is an example artificial neural network (NN). NNs are typically composed of several layers. The leftmost layer in this network is called the input layer, and the neurons within the layer are called input neurons. The rightmost, or output, layer contains the output neurons. The middle layers are called hidden layers, as neurons in this layer are neither strictly inputs nor strictly outputs. A neural network may contain many hidden layers; DNNs are those networks comprising more than one hidden layer.

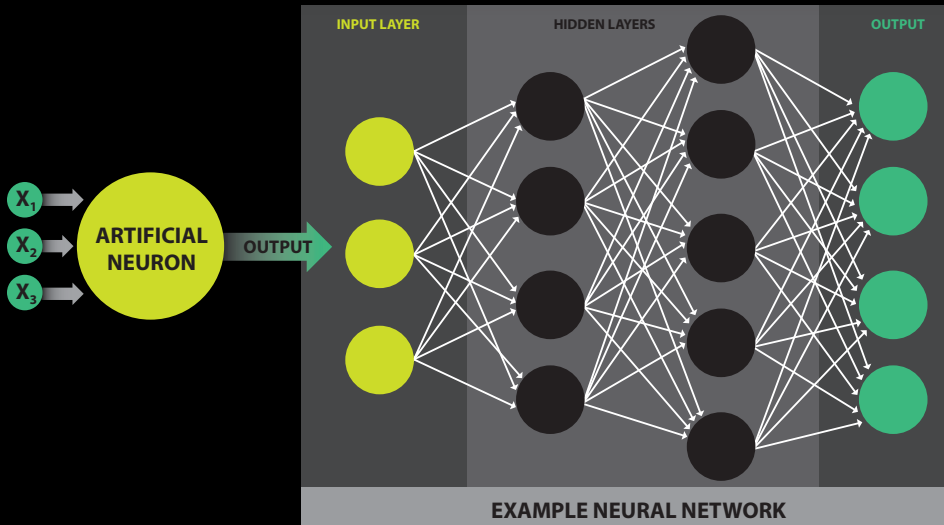


Figure 2: DNNs for Learning Applications.

DNN applications generally employ a two-phase approach. In the offline, or learning, phase, the network ingests large quantities of labeled data to learn some desired task. This type of learning is known as supervised learning. For example, a network attempting to recognize images of cats or dogs would ingest a collection of images with labels indicating whether each picture contains a cat or a dog. The network topology is organized such that the number of output layers corresponds to the number of object classes—in this case, two. Each network node is initialized with a random weight, which is then refined

by repeatedly exposing the network to images of cats or dogs. Weights are adjusted through a process known as backpropagation [4] until the correct node is activated—that is, until the output node value corresponds to either “cat” or “dog.”

The online, or inference, phase consists of simply passing data elements through the previously trained network. Continuing the previous example, the trained network might ingest a picture of a cat not encountered during training. Given a sufficiently diverse training set, the network generalizes the features

underlying the new image to infer that the picture does, in fact, depict a cat.

Convolutional Neural Networks (CNNs)

With increased DNN performance on massively parallel computing architectures (generally) and modern GPUs (specifically), advances in the field have seen performance in ATR tasks rivaling human capabilities [6]. This increase in accuracy is achieved by augmenting traditional DNNs operating on image data with convolution layers that learn to recognize more complex visual features. These improved networks (an example of which is shown in Figure 3) are called CNNs.

To recognize more complex visual features in images, convolutional layers in CNNs apply convolution kernels to each pixel in the input (image) layer. A convolution kernel is a matrix of values encoding weights that are applied to the operating pixel’s nearest neighbors. For example, convolution kernels are used extensively in image processing to sharpen or to blur images. In this case, kernel weights are learned by the network. A convolutional layer thus produces a set of images to which the kernel has been applied. The number

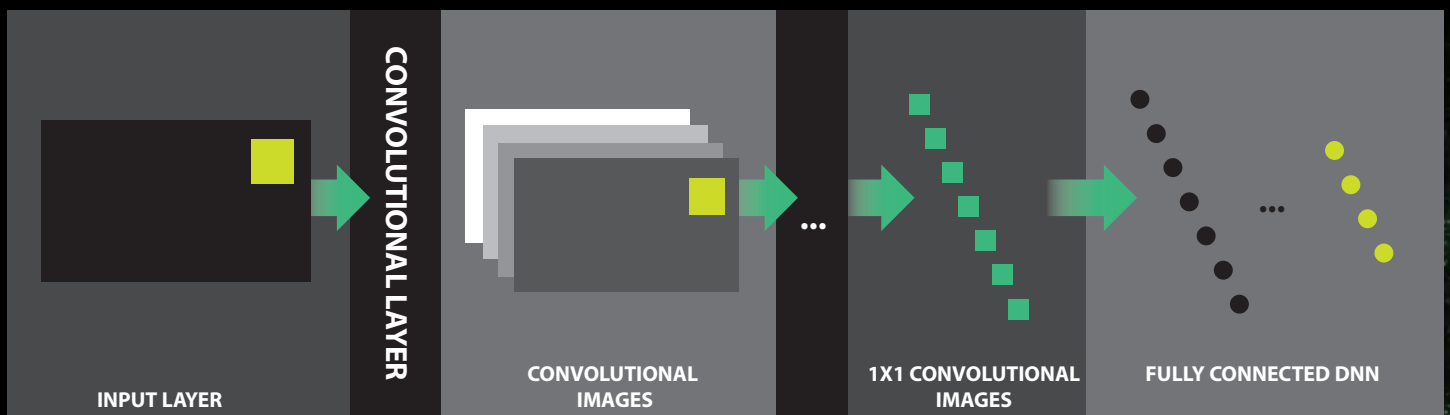


Figure 3: CNN Example.

and size of the convolutional images vary based on the kernel size and overall network topology. Often, this process is applied repeatedly until convolutional images comprising a single pixel are obtained. These 1×1 images then serve as input to a fully connected DNN, which ultimately performs the desired task.

While CNNs are applicable to a wide variety of scenarios, the availability of large, labeled data sets for image recognition has increased the efficacy of CNNs for recognition tasks. For example, these networks power image-based searches and often serve as the visual systems for robotic systems. Recently, NVIDIA demonstrated BB8, a CNN-based autonomous car. The CNN was trained using only 72 hr of human driving data—captured by two forward-facing cameras—and performs exceptionally well in similar, but not exactly identical, driving environments [7]. The ability to generalize underlying features to correctly perform a desired task, as in autonomous driving with NVIDIA's BB8, demonstrates the potential power of CNNs for artificial intelligence (AI) applications.

Recurrent Neural Networks (RNNs)

Success with CNNs in visually oriented applications have spurred advances in audio applications as well. In typical CNN topologies, current inference tasks do not enhance the network's recognition abilities in future tasks. While this lack of impact is not a major concern for certain visual tasks—for example, identifying a cat in an image—information derived from new examples can be highly useful for speech recognition tasks. So-called recurrent neural networks, or those in which current inference tasks inform future tasks, are the key mechanism behind recent

success in speech-to-text recognition applications based on deep learning.

Recurrent neural networks (RNNs) are named for their cyclic topology—namely, the addition of recurrent, or latent, network layers connecting to previous layers. This topology permits current inference tasks to influence the network's performance in future tasks. A schematic of a typical recurrent network topology is illustrated in Figure 4. Note that the particular size, position, and number of recurrent layers vary depending on desired outcomes, but the simple network above demonstrates the fundamental topology. Here the yellow layer cycles back to a previous layer, providing new information based on the data it processes.

A major challenge in speech recognition is the wide variability in human speech

patterns, as well as the presence of background noise. Recently, Baidu Research demonstrated excellent performance with a type of RNN known as long short term memory (LSTM) networks. The second iteration of Baidu Research's system, Deep Speech 2, implements NNs trained with the Connectionist Temporal Classification loss function to predict speech transcriptions from audio [8]. Deep Speech 2 has been trained on 11,940 hr of English and 9,400 hr of Mandarin, and the system works quite well for multiple languages [8]. The ability to use new information derived from current processing tasks—advanced speech recognition, in this case—provides insight into the potential power of RNNs.

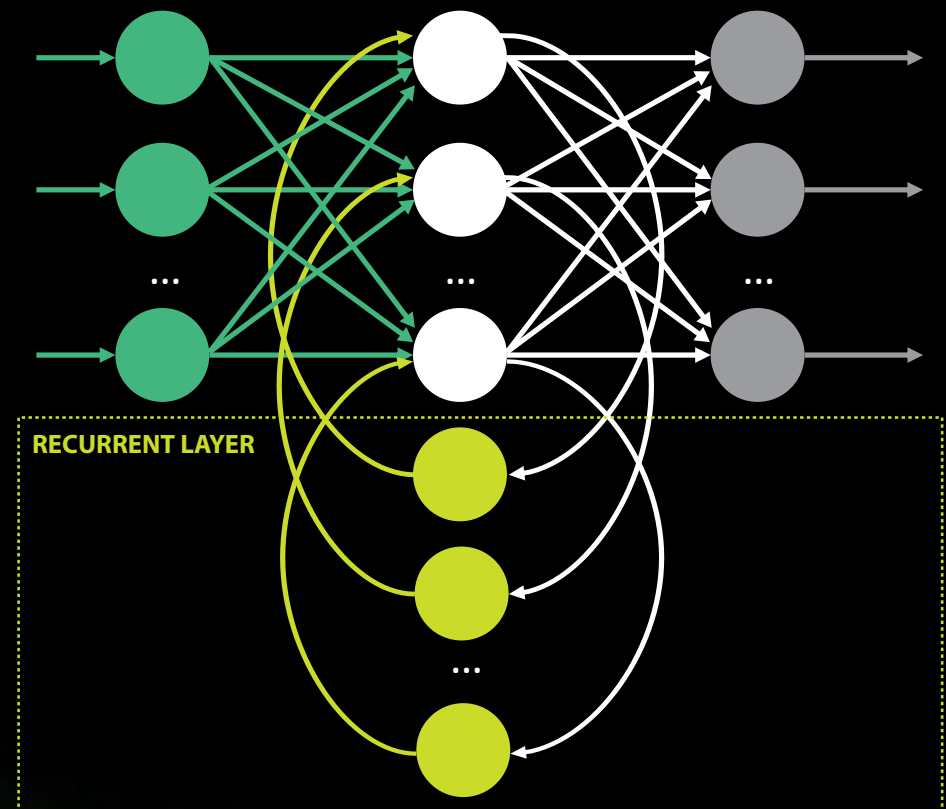


Figure 4: RNN Example.

DNN Organization and Computational Requirements

After witnessing significant advances in the application of CNNs to a wide variety of machine learning problems, several organizations have created software frameworks supporting deep learning research and development. For example, Microsoft provides the Computational Network Toolkit (CNTK) [9], and Google offers TensorFlow [10].

CNTK, TensorFlow, and similar deep learning frameworks provide mechanisms for building NNs, allowing creation of traditional feedforward DNNs, CNNs, and even LSTM networks. To support a variety of topologies, these frameworks structure NNs as directed graphs in which each leaf node represents an input value or parameter and each interior node represents a matrix operation over its children. Such graphs are called computational networks. The computational network in Figure 5 represents a one-hidden-layer sigmoid NN. Generally speaking, the concept of layers as introduced previously is not used in the computational network structure, but the simpler network description tends to enable greater flexibility.

Training requires a cost function to evaluate network accuracy. Numerous possibilities exist, but popular criteria include cross-entropy for classification [9] and mean-square error for regression tasks [9]. In CNTK, for example, the computation network model parameter, W , is improved at each step, t , as:

$$W_{t-1} \leftarrow W_t - \epsilon \Delta W_t,$$

where

$$\Delta W_t = \frac{1}{M_b} \sum_m \nabla_{W_t} J(W; x^m, y^m),$$

and M_b is the mini-batch size, which increases optimization performance. The gradient computation for $\nabla_{W_t} J(W; x^m, y^m)$ is accelerated by storing partial derivatives at model parameter nodes. The network is optimized using a stochastic gradient descent [9] during backpropagation to effectively update W for correct output in an incremental manner. Agarwal et al. [9] provide a complete description of the gradient calculation for various nodes in CNTK.

In the online phase, when model parameters (that is, weight nodes in Figure 5) are known, inference simply requires sequential execution of each vertex in the graph: each node provides an input and an operation to produce its output. When multiple nodes are coupled together, this simple execution model implements advanced NN capabilities.

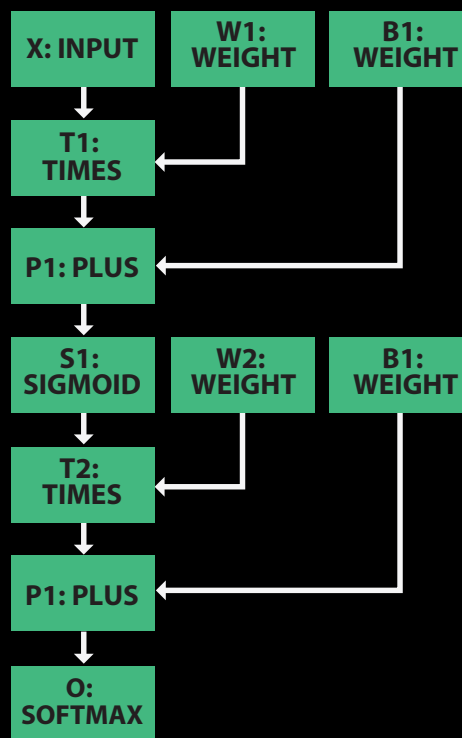


Figure 5: Example Network Encoding One-Hidden-Layer Sigmoid Network.

However, training NNs is difficult on traditional HPC architectures—for example, central processing unit (CPU) clusters—because of significant communication between compute nodes. When the entire network is instead trained on a single GPU, communication latency is reduced, bandwidth is increased, and both physical size and power consumption of compute resources are significantly decreased, particularly when compared to CPU clusters. For example, stochastic gradient descent, a simple but effective training algorithm, executes as much as 40 times faster on a GPU compared to a CPU [3].

This substantial difference results directly from the structure of computational networks: these networks are massively parallel structures, comprising thousands or millions of identical units, each performing the same computation on different data. Importantly, most of these units exhibit no interdependence and can thus be computed simultaneously—that is, in parallel. This execution model, the data-parallel single instruction, multiple data (SIMD) model, matches precisely the underlying hardware architectures of modern GPUs.

GPUS FOR DEEP LEARNING

Recently, NVIDIA has made significant strides in GPU computing for deep learning applications, in both desktop and mobile hardware spaces. For example, the NVIDIA DGX-1 Deep Learning System is powered by Tesla 100 accelerators and trains AlexNet using 1.28 million images with 90 epochs (iterations) in approximately 2 hr [2]. In contrast, a CPU-only implementation requires more than 6 days to train AlexNet under the same conditions.

NVIDIA's Telsa 100 accelerators are based on their newest architecture, Pascal, and are designed specifically for deep learning and AI applications. The Pascal architecture boasts native 16-bit floating point support, resulting in significant speedups for deep learning algorithms. Memory is fast, Chip-on-Wafer-on-Substrate (CoWoS) with High Bandwidth Memory 2 [11], which enables vertical stacking of multiple memory dies. The net result of these architectural features is faster memory accesses than previously achievable. At the same time, connectivity in multi-GPU systems is increased by NVLink, which enables GPU-to-GPU transfers at rates up to 160 GB/s of bidirectional bandwidth. The Telsa P100 GPU boasts 3584 CUDA cores (more than 15 billion transistors) operating at a base clock speed of 1,328 MHz. These extreme capabilities provided by the Pascal architecture enable high-performance DNN training.

In the mobile space, NVIDIA's Tegra line of processors enables fast online inference with trained networks on low-cost and low-size, -weight, and -power (SWaP) CUDA-enabled hardware. For example, NVIDIA's Jetson TX1, which NVIDIA hails to be "the world's first supercomputer on a module," is designed for compute-intensive embedded applications and features an NVIDIA Maxwell GPU with 256 CUDA cores, 4 ARM A57 CPUs with SIMD processing support via ARM NEON extensions, 4K video encode and decode capabilities, and a camera interface capable of 1,400-MP/s throughput. This system is designed for the latest NVIDIA deep learning inference engine, TensorRT, which is used to rapidly optimize, validate, and deploy trained NNs for AI-powered applications. As shown in Figure 6,

Jetson TX1 is roughly the size of a credit card, which allows easy coupling to mobile platforms supporting a wide variety of deployment scenarios, from small unmanned aerial vehicles to large armored vehicles.



	JETSON TX1
GPU	1 TFLOP/s 256-core Maxwell
CPU	64-bit ARM A57 CPUs
Memory	4-GB LPDDR4 25.6 GB/s
Storage	16-GB eMMC
Wifi/BT	802.11 2x2 ac/BT Ready
Networking	1-GB Ethernet
Size	50mm x 87mm
Interface	400-pin board-to-board connector

Figure 6: NVIDIA's Tegra X1 Mobile GPU Platform.

SENTINEL

As mentioned previously, Sentinel is a system that is being developed by the SURVICE Engineering Company to leverage all of these advancements and provide real-time in situ IVA. The system exploits proven methods for data reduction and analysis; object localization, detection, and recognition; and advances in modern computing architectures to support human-in-the-loop deployment scenarios with application to ISR problems in

defense, homeland security, disaster relief, emergency response, and even home security. Despite tremendous progress in both hardware and software support, next-generation computer vision and data analysis systems—such as Sentinel—place high demands on the resources supporting their implementation. The challenges inherent to these systems must be overcome to realize real-time in situ IVA for augmenting and enhancing users' understanding of live data streams.

To exploit the benefits of modern GPUs, programmers must understand and use data-level parallelism carefully and correctly, which is often a difficult and time-consuming task. However, with careful consideration of the low-level architectural features, the SIMD units of modern GPUs offer potentially significant increases in runtime performance across the full range of GPU computing platforms.

For example, as shown in Figure 7, initial results with dynamic mode decomposition (DMD) for foreground/background separation within Sentinel demonstrate significantly better-than-real-time performance [12]. At the same time, Sentinel's ATR capabilities exploit current computational network frameworks to instantiate proven CNN topologies for state-of-the-art detection. Specifically, the system uses the Inception-v3 topology [13] for ATR, capitalizing on the latest GPU computing frameworks to accelerate both training and inference. Integrating these frameworks in Sentinel permits high-performance CNN training on desktop- and workstation-class systems, with trained networks deployed across the full range of NVIDIA GPUs, including its Tegra mobile computing line.

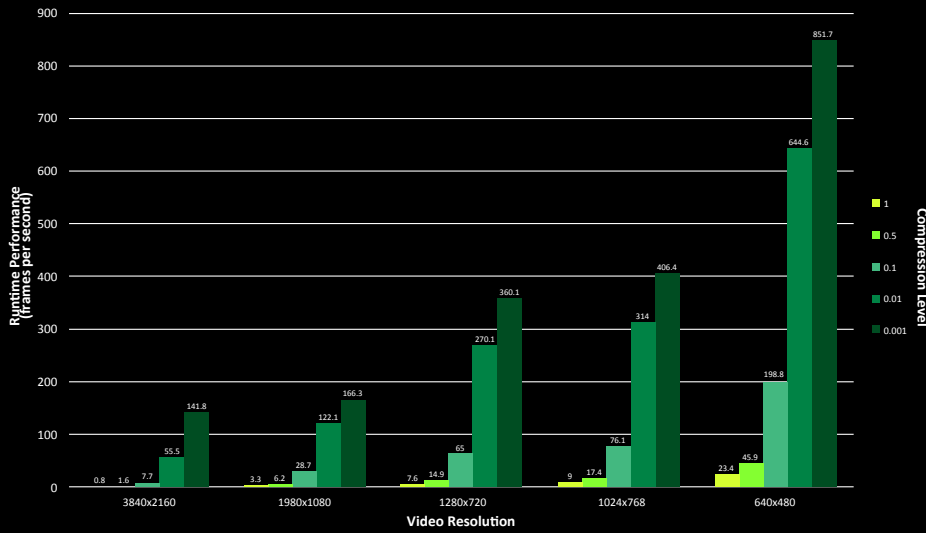


Figure 7: Sentinel DMD-Based Foreground/Background Separation.

Sentinel Performance, NVIDIA Tesla K40c

The performance and flexibility of Sentinel also permits a distributed architecture to support various deployment scenarios. In particular, in situ IVA processing uses the NVIDIA Tegra X1 hardware platform coupled with commercial-off-the-shelf (COTS) sensor hardware to execute core data analysis operations onboard, so that only relevant, actionable information need be transmitted to the primary user interface. As summarized in Figure 8, this distributed architecture enables Sentinel-enabled IVA modules to execute remotely. For example, a Sentinel-enabled IVA module mounted on a UAV can relay customizable battlefield information not only to forward-deployed units but also to analysts or operators at a central location, ultimately resulting in informed decisions regarding possible courses of action.

Real-time in situ IVA provided by the core Sentinel computer vision and data analysis system enables informed decisions based on enhanced understanding of live data streams.

At the same time, the distributed architecture allows Sentinel-enabled IVA applications to span a continuum, from fully centralized for traditional analysis tasks on desktop system, to fully distributed for aerial ISR and other remote sensing scenarios.

Pushing computation to mobile computing architectures has many advantages, particularly in cases where multiple live video streams or other sensor data are monitored in parallel. A distributed architecture

reduces computational requirements at centralized locations and reduces total system failure rates by decoupling system components. In addition, sending only relevant information derived from Sentinel-processed data streams across networks reduces overall communications traffic. These capabilities offer the potential to reduce users' cognitive burden and, ultimately, to improve decision-making in many military and commercial ISR scenarios.

FUTURE IMPACT

The increased efficacy of deep NNs in both image and speech recognition tasks, coupled with increased performance via GPU acceleration, has brought about a resurgence of deep learning techniques. NVIDIA's recent hardware and supporting software frameworks enable the next generation of deep learning applications, such as demonstrated in the Sentinel real-time, in situ intelligent video analytics system. The distributed architecture enables diverse deployment scenarios, ultimately providing means to transmit only relevant, actionable information to interested parties.

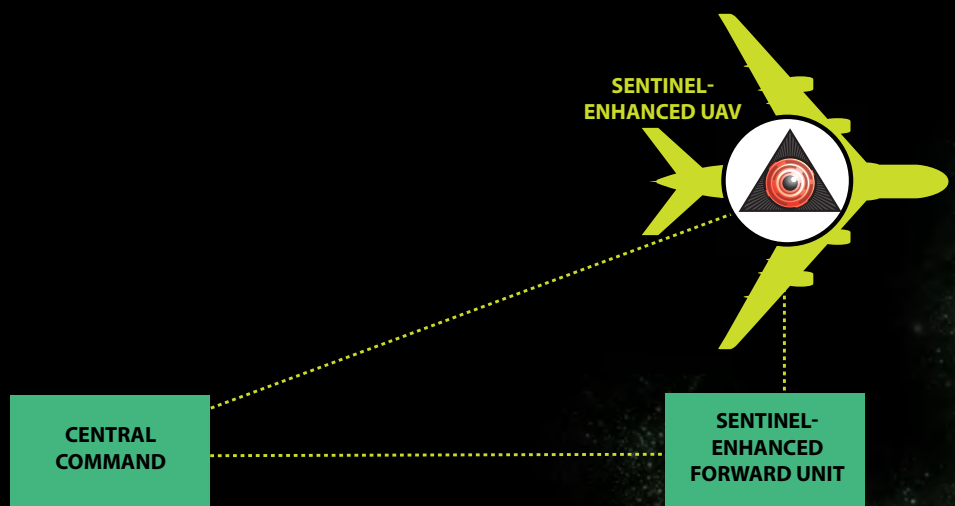


Figure 8: Distributed Architecture Enabling Diverse Operations for Sentinel-Enabled Modules.

Continued advancements and refinements in deep learning may serve as the foundation to high-level task planning AI systems. Already, CNNs control automobiles in a wide variety of driving scenarios—from markerless roads to construction zones to busy highways—while speech recognition systems power companion AI applications on cell phones and other low-cost, low-SWaP platforms. Current deep learning achievements are both important and significant; however, these techniques nevertheless require additional research, development, and, ultimately, coupling with human-like cognitive AI architectures to enable the next-generation applications supporting the modern warfighter. ■

REFERENCES

- [1] Russakovsky, O., J. Deng, H. Su, J. Krause, S. Satheesh, S. Ma, Z. Huang, A. Karpathy, A. Khosla, M. Bernstein, A. C. Berg, and L. Fei-Fei. "ImageNet Large Scale Visual Recognition Challenge." *IJCV*, 2015.
- [2] Krizhevsky, A., I. Sutskever, and G. E. Hinton. "Imagenet Classification with Deep Convolutional Neural Networks." *Advances in Neural Information Processing Systems*, 2012.
- [3] Nemire, B. "CUDA Spotlight: GPU-Accelerated Deep Neural Networks." <https://devblogs.nvidia.com/parallellforall/cuda-spotlight-gpu-accelerated-deep-neural-networks/>, accessed May 2016.
- [4] Goodfellow, I., B. Y. and A. Courville. *Deep Learning*. MIT Press, 2016.
- [5] Rosenblatt, F. "The Perceptron - A Perceiving and Recognizing Automaton." Cornell Aeronautical Laboratory Report, 1957.
- [6] He, K., X. Zhang, S. Ren, and J. Sun. "Delving Deep into Rectifiers: Surpassing Human-Level Performance on ImageNet Classification." *Microsoft Research*, 2015.

[7] Bojarski, M., D. Del Testa, D. Dworakowski, B. Firner, B. Flepp, P. Goyal, L. D. Jackel, M. Monfort, U. Muller, J. Zhang, X. Zhang, J. Zhao, and K. Zieba. "End to End Learning for Self-Driving Cars." 2016.

[8] Baidu Research. "Deep Speech 2: End-to-End Speech Recognition in English and Mandarin." Silicon Valley AI Lab, 2015.

[9] Agarwal, A., E. Akchurin, C. Basoglu, and G. Chen. "An Introduction to Computational Networks and the Computational Network Toolkit." Microsoft Technical Report MMSR-TR-2014-112, 2014.

[10] Abadi, M., A. Agrawal, P. Barham, and E. Brevdo. "TensorFlow: Large-Scale Machine Learning on Heterogeneous Systems." Google Whitepaper, 2015.

[11] NVIDIA. "NVIDIA Tesla P100." NVIDIA White Paper, 2016.

[12] Tu, J. H., C. W. Rowley, D. M. Luchtenburg, S. L. Brunton, and K. J. Nathan. "On Dynamic Mode Decomposition: Theory and Applications." *Journal of Computational Dynamics*, vol. 2, pp. 391–421, 2014.

[13] Szegedy, C., V. Vanhoucke, S. Loffe, J. Shlens, and Z. Wojna. "Rethinking the Inception Architecture for Computer Vision." arXiv1512.00567, 2015.

BIOGRAPHIES

SHAWN RECKER is a principal research scientist at the SURVICE Engineering Company's Applied Technology Operation. He is involved in the application of computer vision three-dimensional reconstruction to various problems. He holds a B.S. in computer science from Grove City College and a Ph.D. in computer science from the University of California Davis.

CHRISTIAAN GRIBBLE is a principal research scientist and the Team Lead for the High-Performance Computing Team at the SURVICE Engineering Company's Applied Technology Operation. He is involved in the synthesis of interactive visualization and high-performance computing. He holds a B.S. in mathematics from Grove City College, an M.S. in information networking from Carnegie Mellon University, and a Ph.D. in computer science from the University of Utah.

CONFERENCES AND SYMPOSIA

JANUARY 2017

2017 AIAA Science and Technology Forum and Exposition

9–13 January 2017

Gaylord Texan

Grapevine, TX

<http://www.aiaa-scitech.org/>

FutureEvents ▶

.....

High Temperature Polymeric Laminate Workshop – SAMPE

23–26 January 2017

Charleston, SC

<http://www.nasampe.org/events/EventDetails.aspx?id=817137>

▶

MARCH 2017

National T&E Conference

6–8 March 2017

San Diego Marriott Mission Valley

San Diego, CA

<http://www.ndia.org/meetings/7910/Pages/default.aspx>

▶

.....

2017 Pacific Operational Science & Technology Conference

6–9 March 2017

Hilton Hawaiian Village

Honolulu, HI

<http://www.ndia.org/meetings/7540/Pages/default.aspx>

▶

.....

SAE 2017 Additive Manufacturing Symposium

14–15 March 2017

Knoxville Marriott

Knoxville, TN

<http://www.sae.org/events/ams/?eid=324666153&bid=1526759>

▶

.....

Directed Energy to DC Exhibition (DE2DC)

27–29 March 2017

Pentagon Courtyard/Rayburn Foyer

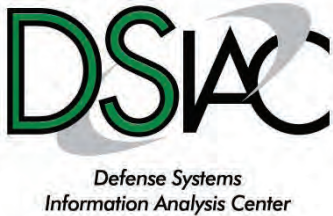
Washington, DC

<http://www.deps.org/DEPSpages/DE2DC17.html>

▶

For more events, visit:

dsiac.org/events/upcoming-events ▶



4695 Millennium Drive
Belcamp, MD 21017-1505



DSIAC ONLINE

www.dsiac.org

DSIAC PRODUCTS AND SERVICES INCLUDE:

- Performing literature searches.
- Providing requested documents.
- Answering technical questions.
- Providing referrals to subject-matter experts (SMEs).
- Collecting, electronically cataloging, preserving, and disseminating Defense Systems scientific and technical information (STI) to qualified users.
- Developing and deploying products, tools, and training based on the needs of the Defense Systems community.
- Fostering and supporting the DSIAC technical Communities of Practice.
- Participating in key DoD conferences and forums to engage and network with the S&T community.
- Performing customer-funded Core Analysis Tasks (CATs) under pre-competed IDIQ Delivery Orders.

DSIAC SCOPE AREAS INCLUDE:

- Advanced Materials
- Autonomous Systems
- Directed Energy
- Energetics
- Military Sensing
- Non-Lethal Weapons
- Reliability, Maintainability, Quality, Supportability, and Interoperability (RMQSI)
- Survivability and Vulnerability
- Weapon Systems

